Increasing the efficiency of simulation-based design explorations via metamodelling

Article *in* Journal of Building Performance Simulation · January 2020

DOI: 10.1080/19401493.2019.1707875

1 author:

Gian Luca Brunetti
Politecnico di Milano

This is a pre-print, pre-publisher's version of the article: Gian Luca Brunetti (2020). "Grafting of design-space models onto models of different scope or resolution". Journal of Building Performance Simulation, *13:3, 227-246. DOI:10.1080/19401493.2020.1712477*

Grafting of design-space models onto models of different scope or resolution

Gian Luca Brunetti [1]

Abstract

Building performance simulation can support parametric explorations of design option spaces. Resources available for modelling and computing often require the reduction of the descriptive information of a design solution at the level of design-space model rather than at that of building model. To obtain that reduction, two design-space models of different scope (for example, one full-scope and simplified, the other partial-scope and detailed) can be combined to make their responses usable as surrogates of those produced by a full-scope detailed inquiry. But aligning two building models of different scope can be difficult and sometimes impossible. This article presents a design-space "grafting" technique supported by metamodelling that makes it possible to hybridize two non-aligned design-space models so as to obtain a diffusely calibrated conjoint response. The strategy can be integrated into metamodelling and decomposition-based optimization to decrease the information costs entailed by parametric explorations.

Keywords: subspace grafting, k-nears neighbour, metamodelling, optimization, model reduction

[1]Department of Architecture and Urban Studies (DAStU), Politecnico di Milano.

Email: gianluca.brunetti@polimi.it.

Grafting of design-space models onto models of different scope or resolution

1. Introduction

The greatest challenge in exploring a building design option space is confronting the "curse of dimensionality" (Bellman, 1957), deriving from the fact that the size and complexity of an option space increase exponentially, at the power of the number of parameters involved. Building designers usually deal with the necessary problem reduction implicitly, by intuition, but the increasing adoption of generative design procedures creates the opportunity to deal with problem reduction explicitly, along a path towards closing the acknowledged gap (Bleil de Souza, 2012) between the tentative approach of building designers and the analytic one of building simulationists.

At the analytical level, the issue of dimensionality can be addressed by several kinds of approaches explicitly or implicitly aimed to reduce the design-space size: optimization, metamodelling, and building model ("scene-model", including the neighbourhood scale) reduction. Optimization can reduce the number of samples (simulations), metamodelling can reduce the sampling costs, and scene-model reduction can reduce the descriptive information of samples.

In the context of optimization, problem reduction can be pursued by the means of scene-models of cascaded scope and resolution, usually organized in such a manner that the smaller the scope, the higher the resolution, so as to make it possible to base general decisions on complete and low-resolution models, and detailed decision on partial and high-resolution ones. But problem reduction can also be pursued by utilizing scene-models of different scope or resolution even outside the context of optimization. This can be done by combining the response of the two (or more) design-space models and aligning them in such a manner to make them usable interchangeably. However, the techniques that are available to align the responses of different design-space models are presently limited to the calibration of scene-models, which is not entirely satisfactory for models of different scope, i.e., having an inner structure lacking a point-to-point correspondence. When two scene-models have a different scope, they indeed lack the correspondences which are necessary to generate a conjoint design-space model, and this reduces the likelihood that they can be mutually calibrated in absolute and relative terms simultaneously.

This paper presents a novel technique that makes it possible to merge the performance predictions produced by two concurrent scene-models of different scope without requiring a preliminary calibration between them, while nevertheless obtaining conjoint calibrated responses. In this technique, the integration of design-space models does not take place at the level of performance predictions (i.e. at the level of independent variables), but at the level of design-spaces (that is, involving the whole range of variables, including the independent ones). This result is obtained by performing a diffuse and progressive point-to-point “grafting” of a problem into another by means of an ad-hoc gradient-based metamodelling technique of the k-nears neighbour type. For doing that, a partial metamodel is built on the basis of samplings performed in the design-space model which is going to receive the “graft”, then another metamodel is built to fill the missing parts by utilizing the gradients metamodelled from the samplings performed in the design-space model contributing the graft.

The case study presented in this article aims to demonstrate, by means of comparisons with the results obtainable through alternative strategies, that: (a) the descriptive information reduction made possible by the grafting technique can produce levels of design-space model reduction comparable with those obtainable with the technique of subspace metamodelling by sequential decomposition; and (b) the conditions exist for combining the grafting technique with the strategies of scene-model reduction, metamodelling, and search-space decomposition in a coherent whole, so as to increase the return of investment on descriptive information without excessive costs in terms of predictive reliability.

1.1. Interdisciplinary literature bases

The foundations of this research are interdisciplinary: they span from constraint propagation to metamodelling, and from calibration to scene-model reduction and system decomposition.

At the core of the capacity of parametric modellers and BIM applications to manage design explorations, there is constraint propagation (Woodbury, 2010; Jabi, 2016; Faloutsos, 2001), which is a process inducing a chain of transformations in a system on the basis of some rules following a triggering event (Sutherland, 1963; Sussman & Steele, 1980). With the aid of constraint propagation, carrying out the exploration in Fig. 1A, for example, would not require imposing three transformations (regarding width, depth and height), but two (width and depth), plus one constraint (i.e. the floor area is constant). The advantages of this strategy become huge in complex problems (Medjdoub & Chenini, 2015) and make constraint propagation essential in a wide range of cases, spanning from characters in animations (Koenig & Varoudis, 2016) to BIM models (Singh, Sawhneya, & Borrmann, 2015). This transformative ability is highly programmable (Wortmann & Tunçer, 2017, Harding, 2017; Dino, 2016) and opens the way to integration with building simulation tools (Ahn et al. 2014; Habibi, 2017); but managing long tool-chains creates brittleness (Jin et al. 2019), which is commonly addressed via the creation of frameworks (Gu et al. 2013; Crawley et al. 2008; Gu et al. 2013; Rahmani, 2015; Kim et al. 2016; Gerrish et al. 2017; Shadram & Mukkavaara, 2018).

A consequence of the link between parametric applications and simulation programs is that of further increasing the already huge importance of models in the architectural domain, along a path which in modernity has at first addressed structural problems (Dong, 2017; Nervi, 1954; Cowan et al. 1968), then environmental analyses, ranging from winds (Davenport, 1960) to solar radiation (Olgyay & Olgyay, 1957) and daylighting (Lam, 1986). In all these situations, the models surrogate something. They surrogate the “real” architectural objects directly or indirectly, by surrogating some models that surrogate the real objects. This is also the meaning in which the term “metamodel” is today used in engineering: an abstract model surrogating abstract relations: often, a computation engine (for example, a neural network) surrogating the action of a more resource-demanding simulation engine (Wang & Shan, 2006).

A criterion for the classification of metamodelling approaches is based on the distinction of the so-called parametric methods, like regression on polynomials (Myers, Montgomery & Anderson-Cook, 2009; Giunta & Watson, 1998) (requiring prior knowledge of a problem’s structure) from the non-parametric methods, like the k-nears neighbours strategy (Altman, 1992), kriging (Gaussian process regression) (Matheron, 1973), radial basis functions (Hardy, 1971), multivariate adaptive regression spline (MARS) (Friedman, 1991), support vector regression (Cortes & Vapnik, 1995; Tang et al. 2019), random forests (Breiman, 2001), and artificial neural networks (Cheng & Titterington, 1994).

The usefulness of a metamodelling – for example, for increasing optimization efficiency (Wortmann et al., 2015) - is highly dependent on the kinds of problems addressed (Jin, Chen & Simpson, 2001; Villa-Vialaneix, 2014) and can be improved by integrating information about the gradients between vectors (Keulen &Vervenne, 2004; Laurent, 2019).

By applying calibration to metamodelling, the relations between building simulation and calibration, which are usually measured at the level of scene-model instances (Coakley, Raftery & Keane, 2014) are extended at design-space level. Sophisticated knowledge-based procedures have been developed for that task (Pedrini, Westphal & Lamberts, 2002; Yoon, Lee & Claridge, 2003; Raftery, Keane & O’Donnell, 2011a, 2011b), as well as methods derived from optimization (Reddy, Maor & Panjapornpon, 2007a, 2007b; Coakley et al. 2011) and, more recently, bayesian logic (Monari & Strachan, 2017).

Scene-model reduction (a very active research topic) is of concern for this research because it can substantially decrease model complexity. Strategies for reducing the complexity of thermal models have been proposed by Kim and Braun (2015) and Deng et al. (2014); criteria for measuring the computational load spared at micro-urban-scale by model reductions have been proposed by Heidarinejad et al. (2017); residential model reduction has been pursued in De Rosa et al. (2019); a combination of model-order and descriptive reductions has been performed by Shamsi et al. (2017) and Kim et al. (2014); and the effects of combining model reduction and optimization-induced reduction have been pursued by Gouda, Danaher & Underwood (2002).

System decomposition is an essential component of optimization techniques like Dynamic Programming (DP) (Bellman, 1957; Bertsekas, 2017a, 2017b; Radford & Gero, 1988), block-coordinate descent (BCD) (Tseng, 2001; Bertsekas, 1999), multidisciplinary design optimization (MDO) (Cramer et al. 1994; Geyer, 2009), and of the systemic approaches, including systems engineering (SE) (Gosling, 1962; Weinberg, 1975; Sage, 1992; Pimmler and Eppinger, 1994; Choudhary, Papalambros, & Malkawi, 2005). DP and BCD allow for overlaps between subspaces; in MDO, decomposition follows the compartmentalization of knowledge; and SE admits various alternative criteria to decomposition, like that of functional system, or “Aspect”, linked to the quantification of performances on the basis of the contribution to a certain system’s behaviour (Augenbroe, 2019; De Wilde, 2018). MDO and SE intersect in the multimethodology approach (Mingers, 1997) and in the multimodel approach (Fishwick and Ziegler, 1992). Within the systemic approach, the role of decomposition is particularly central in the contributions by Simon, where it is supported by the concept of near-decomposability (1962, 1973). To the importance of decomposition in SE, contributes the increasingly prominent role that modelling and simulation play in it (INCOSE, 2019, Bachman, 2003, Geyer, et al. 2003).

2. Methodologies

2.1. The technique of design-space grafting

The operation of combining a full-scope simplified design-space model and a reduced-scope detailed one in a design exploration can be facilitated by the ability to hybridize them in a manner suited to make the derived model adequate to surrogate the full-scope detailed one. But currently, there is no strategy available for doing this: the hybridization cannot indeed be performed simply by inserting the subspaces into the design-space “receiving” the information, because the original design-spaces may be shaped in ways that prevent the possibility of preserving the integrity of their internal relations in the merging operation. What would indeed have to be merged in that situation would be the two design-space models, not just the performances of the two scene-models after calibration. The latter operation may be attempted, for example, by merging the performances of a few rooms into some whole-building performance predictions.

The problem with the described strategy is that it cannot be performed if the scene-models have not been (or cannot be) mutually calibrated; which can easily happen when they are complex and/or full of higher-order relations. The responses of a room, indeed, like one of the two shown in Fig.3D2 or Fig.6C, can be irreducible to the responses of a system of rooms (Fig.3A or Fig.6A).

The novel possibility introduced by the “grafting” technique is that of making it possible to mix design-space models of different scope at the level of their entire range of vector components, rather than only at the level of performance predictions. This does not require mixing the responses of each room instance produced in a parametric exploration into the response of the corresponding building instance, but merging adaptively and in a point-to-point fashion the whole range of the performances of the room instances into the whole range of performances of the building instances.

The preliminary operation for merging two design-space models of different scope is to create a complete point-to-point correspondence between them. However, when a design-space has a smaller scope than another one, its parametric description utilizes fewer parameters, which prevents the possibility of hybridization, because that possibility exists only between series having the same topology (homotopical). To circumvent that issue, additional “dummy” parameters must be added to the smaller-scope design-space.

The grafting technique in question utilizes as the basis for deriving new vectors the known vectors that are going to receive the graft in the “receiving” space from an “auxiliary” design-space model (“donor” space), and utilizes the known near-neighbouring gradients derived from the donor space as the means for deriving the new vectors in the receiving space. The operation is performed with the aid of a novel ad-hoc gradient-based metamodelling procedure of the k-nears neighbour family (here named DWGN: distance-weighted gradient network) suited to address combinatorial problems.

In this framework, the existing vectors in the receiving space constitute the “anchors” from which the position of the newly derived vectors is going to be determined, by means of the gradients; and the existing vectors in the donor space constitute the information from which the gradients are derived. The concurrency involving the vector candidates makes it possible to transfer the information regarding the curvatures of the donor space into the receiving space in a layered and diffusely-fit manner, biological-like, not surgical-like.

The new vectors in the receiving space are calculated in the following manner:

$$x_{u_i}=\mathrm{x}_{k_i}+\mathrm{x}_{k_i} * \frac{\sum_{i=1}^{n} \mathrm{GradW}_{\mathrm{knn}_i,\mathrm{unn}_i} * \frac{1}{d_{x_{u_i},\mathrm{x}_{k_i}}}}{\sum_{i=1}^{n} \frac{1}{d_{x_{u_i},\mathrm{x}_{k_i}}}},$$

where:
x_{u_i}: unknown vector in the receiving space at iteration *i*;
x_{k_i}: known vector in the receiving space;
$d_{x_{k_i},\mathrm{x}_{u_i}}$: distance between a known and an unknown point in the receiving space;
$\frac{1}{d_{x_{k_i},\mathrm{x}_{u_i}}}$: weight assigned to the vector: the inverse of its distance;
$\mathrm{GradW}_{x_{k_i},\mathrm{rknn}_i,\mathrm{runn}_i}$: gradient in the donor space between a near-neighbour of the known vector in the receiving space (x_{rknn_i}) and a near-neighbour of the unknown vector (x_{runn_i}), weighted with respect to the distance from the known vector.

Each gradient is weighted in the following manner:

$$\mathrm{GradW}_{\mathrm{knn}_i,\mathrm{unn}_i} = \frac{\sum_{i=1}^{n} \mathrm{Grad}_{\mathrm{knn}_i,\mathrm{unn}_i} * \frac{(\frac{1}{d_{x_{u_i},\mathrm{x}_{\mathrm{knn}_i}}})+(\frac{1}{d_{x_{u_i},\mathrm{x}_{\mathrm{unn}_i}}})}{2}}{\sum_{i=1}^{n} \frac{(\frac{1}{d_{x_{u_i},\mathrm{x}_{\mathrm{knn}_i}}})+(\frac{1}{d_{x_{u_i},\mathrm{x}_{\mathrm{unn}_i}}})}{2}},$$

where:
$\mathrm{Grad}_{\mathrm{knn}_i,\mathrm{unn}_i}$, candidate gradient component between a near-neighbour of a known vector in the receiving space (knn_i) and a near neighbour of an unknown vector (unn_i), at *i*;

$\frac{(\frac{1}{d_{x_{u_i}, \mathrm{x}_{\mathrm{knn}_i}}})+(\frac{1}{d_{x_{u_i}, \mathrm{x}_{\mathrm{unn}_i}}})}{2}$: weight attributed on the basis of the inverse of the average distance of the vectors from which the gradient is derived from the vector to which it is going to be applied.

Let us now examine how the technique works in an example viewable in 3D (Fig.1) featuring 2 independent variables (x, y) and 1 dependent one (z). For simplicity, the boundaries between the receiving space and the donor space have here been set up so that they “cut through” a hyperplane, while, typically, they are set between hyperplanes.

Let us suppose that a part of the design-space model shown in Fig. 1A is going to receive the graft of the design-space model shown in Fig. 1C. The first step of the grafting procedure is that of removing the parts of the receiving model which have to be substituted (Fig. 1B). The second is extracting a collection of the gradients from the donor space (Fig. 1D). The third is applying those gradients (by distance-weight-averaging them) to the most peripheral vectors of the receiving space adjacent to unknown ones, so as to model the additions to the receiving space considering the curvatures that are present in both spaces (Fig.1G). Fig. 1E shows the candidate vectors created from the gradients along the y axis, and Fig. 1F does that as regards the x axis. If, after one procedure cycle, some vectors remain unknown, a new cycle is performed, including the newly derived vectors in the receiving space - on and on, until no unknown vectors are left.

Fig. 1. An example of a procedural sequence for grafting a partial design space model onto another.

2.2. Requirements for the transformation of scene-models

Constraint propagation can support the capability of CAD programs to generate myriads of model instances (Nembrini, Samberger, Labelle, 2014) and of imposing transformation cost as an aspect of optimal design (Abdelalim, O'Brien & Shi, 2017), but is not sufficient, by itself alone, to guarantee transformability, which depends indeed on the degrees of freedom of a model (Daverman, Sher, 2001). A transitional model that is only expected to mutate with regard to the length of its edges (Fig.2B), for example, does not have to be different from an ordinary model:

its mutation can take place in conditions of constant configuration. But whenever a model is required to be mutated in its configuration (as regards, for example, the number of its faces or edges) it has to be conceived so as to embody redundancy ("degeneracy" - Sussman, 2007) and possess all the configurational qualities needed in the subsequent morphing steps, as a sort of least common multiple of all the possible model states. Fig.2C is an example of transformation in constant configuration. In Fig.2D, a model similar to that in Fig.2B is mutated in variable configuration; and in Fig.2E, the same mutation is performed in constant configuration.

Having conditions of constant configuration in a transformation governed by constraint propagation can substantially simplify the transformation itself, compelling it to take place as a quantitative-only process rather than a qualitative-and-quantitative one. On the other hand, constant configuration reduces the degrees of freedom available to transformation, to the point of making transformation impossible beyond certain levels of complexity.

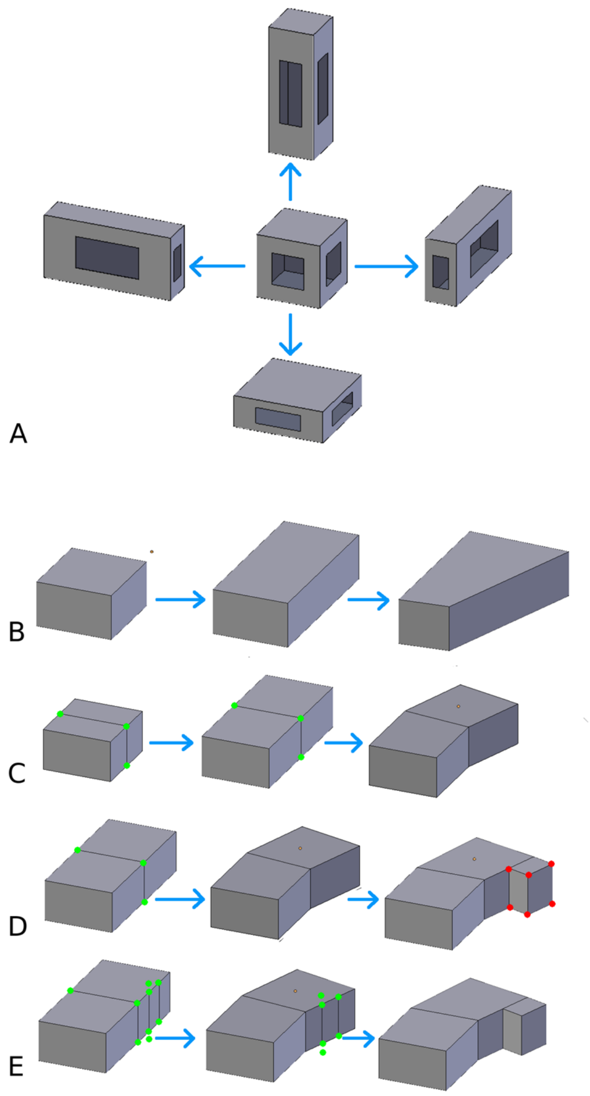

Fig. 2. A. Constraint propagation in conditions of constant volume. B, C) Transformations not requiring configurational (topological) changes. D) Transformations in conditions of variable configuration. E. The same transformation as in (D), but in constant configuration. In green: redundant vertices aimed to obtain homotopy. In red: addition of new vertices.

2.3. Problem decomposition as a strategy for reducing search size

A strategy for bypassing the difficulty of transforming scene-models in variable configuration is that of abandoning constant configuration only intermittently, by organizing the explorations in cascades, introducing discontinuities, “leaps”, between transformation phases carried out in constant configuration. Concentrating transformations is indeed simpler than distributing them uniformly; but assuring the condition of constant configuration within the subspaces may require charging the scene-models with a content of abstraction (aimed to create the required redundancy) higher than that of ordinary models.

The “cascades” in question can be organized as a succession of subspace searches that: (a) may regard different parts of the design-space, (b) may have different resolutions, (c) may have an only partially overlapping scope, (d) may pertain to different performance domains, and/or (e) can be modelled by means of several alternative decomposition-based approaches, like dynamic programming (Bellman, 1957; Bertsekas, 2017a, 2017b; Radford & Gero, 1988) and block-coordinate descent (Tseng, 2001; Bertsekas, 1999). In building-simulation-supported design, however, the strategy of cascading the explorations is disincentivized by the fact that, because energy models are usually based on zonal criteria (i.e. thermal zones at homogeneous air temperature), many export procedures from parametric modellers to simulation programs encourage the assignment of one zone per room (Kim et al. 2015), relying on a point-to-point correspondence between architectural objects and thermal models, in a manner that is not unrelated to the tendency to overspecifying scene-models in the preliminary design phases (Cole, Hale & Edgar, 2013), like in Fig.3A.

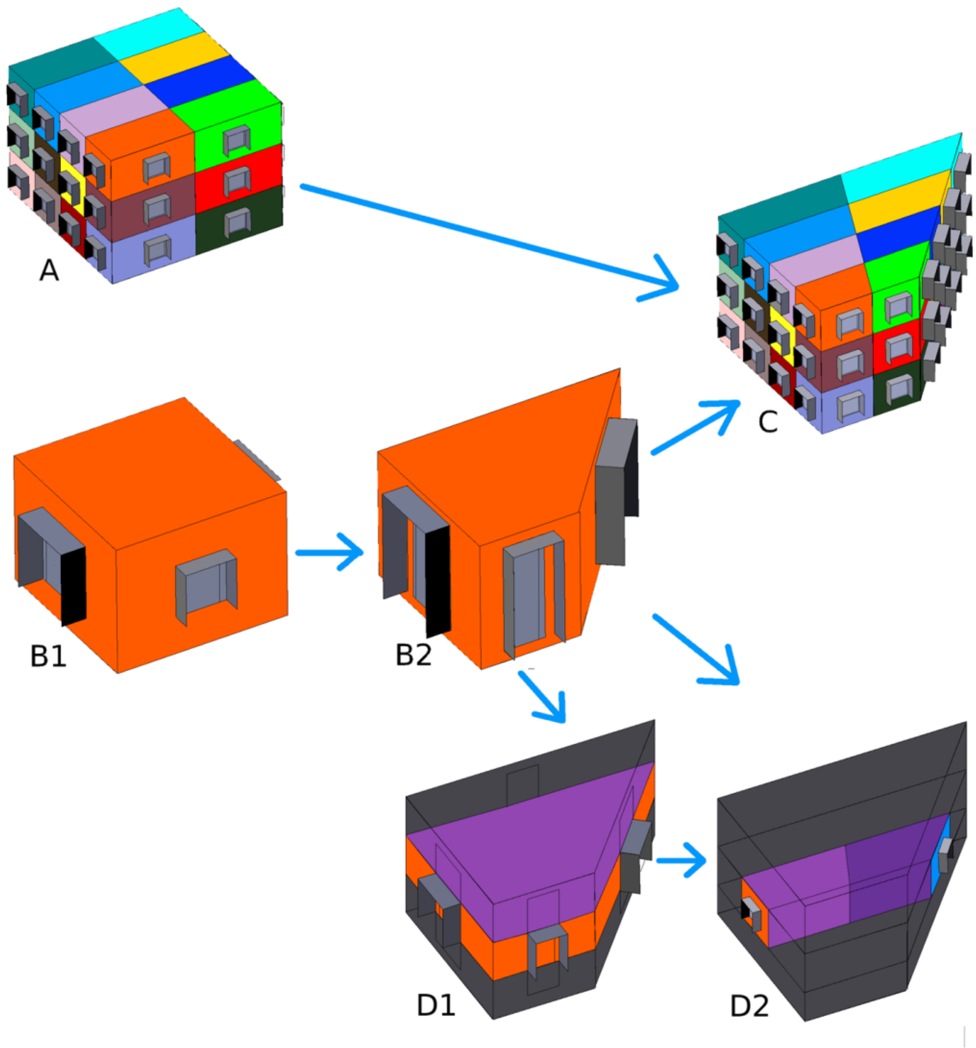

Fig. 3. Example of alternative transformation paths. Each thermal zone has been assigned a different colour. The surfaces in violet are set to adiabatic. Path A-C: transformation in conditions of constant configuration and high resolution. Path B1-B2-C: transformations of increasing resolution and variable configuration. Path B1-B2-D1-D2: transformation of increasing resolution, decreasing scope and variable configuration.

Simplicity can be a good heuristic indicator of the cognitive and information load related to a model; but a reduction of the information load is not always a good thing (Sweller, 1988). For example, a reduction of the information load linked to a certain problem may correspond to an increase of the cognitive load necessary for understanding the structure of the redefined problem, which happens whenever the complexity of a final design scheme is assumed since the early exploration phases (Fig.3A). Bringing the structure of a design problem into the foreground would require the introduction of additional content of abstraction into the building models and the deletion/reduction of many point-to-point correspondences; which in current BIM programs would require “intelligent” procedural libraries of the type envisaged by Sacks, Eastman & Lee (2004), but oriented to abstraction, rather than specificity.

An example of a cascaded search scheme of increasing resolution suited to avoid representing design problems literally is shown in Fig.3-B1-B2 and B1-D2. The search path B1-C is the cascaded equivalent of A-C, entailing increasing modelling resolution and constant scope. The strategies in B1-B2-D1-D2 and B1-B2-D2 constitute other cascaded constant-configuration alternatives to A, structured along exploration phases of increasing resolution and decreasing scope. In B1-B2, a shape representing the whole volume of a building is modified; in D1, only one story is taken into account; and in D2, a minimum unit composed of two back-to-back rooms is assumed for finer decisions.

2.4 Criteria for knowledge-driven scene-model reduction

To be suited to support a sequentially-decomposed exploration, a scene-model should focus on the most sensitive parameters into play and drop the inessential information. In Fig. 3, the reduction from case 6C to 6B1-B2 entails an aggregation of the zones and the co-planar windows, partitions, floors and envelope surfaces. In a simulation tool conceived for approximated design, those reductions would not entail weakening the correspondences between the object and the model; but in a tool conceived for detailed design, they would - and the group of instances related to Fig. 3C requires such a tool. This issue stems from the fact that, because in a high-resolution program, the definition of building “objects” (floors, partitions, windows...) is literal, the objects compounding other objects (like, for example, the openings derived by aggregation of other openings in Fig. 3B1 and 3B2) would be interpreted as non-abstract, over-sized objects; which in turn would generate a distortion of the mutual thermal relations between entities, ultimately deriving from the fact that any change in size regards lines, surfaces and volumes in accordance to different relations (Thompson, 1917-1942) (respectively, linear, quadratic, and cubic: the faces of a cube increase at the square power of an edge, and the volume at the cubic power). The “compaction” of smaller objects into larger ones (even more when coupled to changes in shape, like in Fig.3B1 and 3B2) alters, indeed, the simulated thermal processes in myriads of manners, involving a wide range of phenomena (from stack effect at building and/or story level to solar access, from solar gains to radiant processes), hindering calibration.

However, the goal of simplifying a scene-model is not necessarily that of making it as faithful as possible to the original: it may also be that of making it specifically appropriate to a certain design exploration (which requires a kind of domain knowledge that is still not yet embodied into simulation tools), even at the cost of making it less appropriate for other explorations. The scene-model in Fig.3B1, for example, is more suited to convey information regarding solar access than that in 3B2, because it retains the same width-to-height proportions of the original 3C1; while the model in 3B2 is more suited to convey information deriving from the stack effect at building level, because it retains the original total window height.

It should also be noted that decomposing problems by reduction is not the only possible strategy. Problems can also be decomposed by reformulation, as it happens in Yang et al. (2018), aiming to make optimization strategies more attuned with physical representations; or in Welle, Rogers & Fischer (2012) targeting the lighting domain. But problems can also be decomposed for the pure sake of the search, as in decomposition-based optimization.

2.5 Problem reduction through search

The way problems are decomposed influences how they can be solved (Gralla, Herrmann & Morency, 2019; Brown and Mueller, 2019), but the inflexibility of current scene-models discourages designers from decomposing problems preliminarly (Turrin, von Buelow and Stouffs, 2011; Ercan and Elias-Ozkan, 2015). Today’s most popular optimization methods – that primarily involve metaheuristics, like genetic algorithms (Deb et al. 2002: Yang and Bouchlaghem, 2010), particle-swarm optimization (Boudjehem and Boudjehem 2017, Cao et al.

2017) and simulated annealing (Al-Bazi and Dawood, 2018) - do not indeed require that problems are explicitly decomposed (Evins, 2013; Kheiri, 2018).

Expert knowledge can contribute to the decomposition of problems and their parametrization, but in problems which are given a flat, monolithic structure, parametrization and decomposition are essentially the same thing.

Some degrees of flexibility are made possible by the fact that, in building design, a parameter can embody various orders of abstraction and complexity and represent a wide range of things, from the quality of an object (like a glass thickness) to a performance (like lighting levels), and the fact that the meaning of entities can also depend on scale and context (with the consequence, for example, that a surface can define a wide range of things, from a window glazing to a city boundary layer). But further flexibility should be sought in the search process itself, considering that, whatever the assessment approach (intuitive or expert reasoning, automated exploration...), when simulation is involved, the search is direct, test-based (Lewis, Torczon & Trosset, 2000).

For addressing the relations between decomposition and search, reference can be made here to the most basic search strategies, breadth-first search and depth-first search, which can be represented as tree structures (Winston, 1992). The kind of search which is more suited to a preliminary exploration is, notoriously, breadth-first search, which requires that the leaves attached to some intermediate nodes are explored, and returns a general view of the model's responses (Fig.4A).

Depth-first search is less suited to preliminary investigations, because it produces high-resolution local information by working on a “deep” part of the search tree at a time. It would indeed be suited to explore only a fraction of the design-space explorable with a breadth-first search for the same number of iterations (Fig.4B). Performing breadth-first search, however, is difficult when a “literal”, point-to-point approach to modelling is adopted: if a search is direct, it is based on a single scene-model (instance) at a time; and if the description of the object is literal, there are no leaves at the intermediate nodes, and in facts at any node: all the leaves are peripheral. While what is needed for a breadth-first search are leaves located at the intermediate nodes of the search-tree, which are the ones representing families, groups of instances - like in Fig.3B1, 3B2 and 3D1.

Lacking these, a solution to explore a design-space evenly and economically is that of sampling a reduced but well-distributed group of instances by varying one parameter at a time in a star sampling (Moustapha et al. 2018); which can be a powerful approach (Frey, Engelhardt & Greitzer, 2003), but is exposed to the risk of inconstant quality of results, because choosing parameter levels appropriately requires expert knowledge (Björklund, 2013; Yu & Honda, 2016).

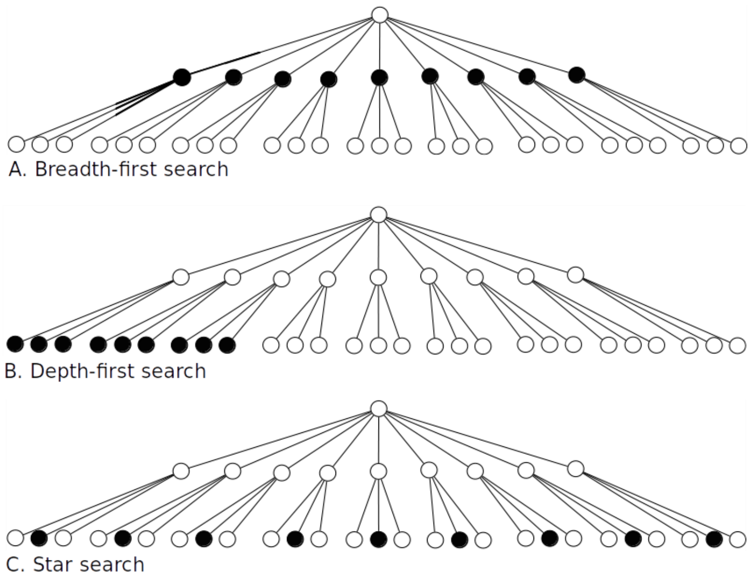

Fig. 4. Three primary types of search. In black: the explored instances.

Locating the leaves of the search-tree at the intermediate nodes in a breadth-first search would require to represent the instances at such nodes more abstractly than those at the peripheral leaves (Fig. 3B1 and 3B2); it would require to define correspondences between the simplified representation of a problem and the detailed one, and would return in exchange the possibility to structure a search so as to give to it different levels of abstraction/resolution (Fig. 3B1-3C) and/or scope (Fig. 3B2-3D1, 3D1-3D2) and widen the possibilities of parametric iteration (Ercan & Elias-Ozkan, 2015; Wynn & Eckert, 2017).

2.7. Case study

In the here presented case study, the outcomes of design-space grafting were compared with those of other forms of surrogation, like metamodelling and search decomposition, by putting in relation the reduction of the amount of descriptive information made possible by each strategy with the increase of approximation caused.

To that end, a hypothetical case study was set up rather than a concrete one, so as to increase the likelihood of obtaining saddle curvatures in the response surfaces and tighten the stress-test conditions of the modelling and optimization criteria. The objective of saddle curvatures was pursued by positioning a large solar obstruction in the middle of the solar access field of the building – an un-specific three-stories-high building composed of uniformly-sized back-to-back rooms, suited to represent a wide range of types.

The design problem was aimed to define the shape and position of the building in its plot so as to maximise the free-floating average resultant temperatures in February; while the ultimate objective of the inquiry was that of assessing the predictive reliability linked to each exploration technique and the returns on investment of the descriptive information involved in each exploration “trail”.

In total, four alternative scene-models were taken into account (Fig.6): 1) the full-scope (whole building) detailed (high-resolution) model (Fig.7A), assumed as a reference; 2) a full-scope low-resolution (single-zone) model (Fig.7B); 3) a reduced-scope (two rooms) and full-resolution (two detailed zones) model (Fig.7C); 4) a reduced-scope (two rooms) and low-resolution (one simplified zone) model (Fig.7D).

The reference model could be composed of 1, 2 or 3 stories and, 6, 12 or 18 thermal zones, being each story constituted by 6 zones. The transformations between instances took place partially in conditions of variable configuration (depending on building height) and partially of constant configuration. Constant configuration was instead always maintained in the transformations regarding the simplified full-scope model, which was adapted to the changes in height by allowing its floors the possibility of assuming infinitesimal dimensions, so as to make their thermal influence negligible while avoiding topological modifications. The reduction undergone by the simplified model aimed to decrease the number of entities (vertices, surfaces, zones) into play.

The strategies through which the detailed full-scope model was converted into the simplified one were based on joining all the co-planar surfaces sharing vertices and edges, and on compacting the windows on each facade into an opening of equivalent total area and same total height, obtaining a configuration similar to those in Fig. 3B1 and B2. This was done in the passage from the distinct windows for each story in the examples in Fig. 6A and 7A to the unified windows for the whole height in Fig. 6B and 7B. With the same criteria, the vertical partitions extended themselves from top to bottom of the building without touching the envelope, and similarly did the floors along the building width and depth. The vertical partitions and the walls met without intersecting each other and without exchanging heat by conduction. These choices further weakened the thermal correspondence between the detailed models and the simplified one (see section 2.1) and strengthened the premises for a lack of calibration between them.

The reduced-scope detailed model (Fig.7C), representing the minimum average building unit, was constituted by the central back-to-back zones of the three-stories version of the building, set with adiabatic boundary conditions towards the other rooms (like in Fig.3D2).

The reduced-scope simplified model (Fig.7D) differed from the detailed one in the fact that the two rooms were modelled as a unified thermal zone having the interior partition disjoint from the other surfaces, in a manner similar to those of the simplified full-scope model.

The transformation of the number of stories and, therefore, height, of the two full-scope models took place in conditions of constant volume, with the consequence that the higher the building was, the smaller its floor area (like in Fig.2A).

The transformations undergone by the full-scope detailed model were the following (Fig.5, 6): A) variation in height (3 levels); B) variation of the width-to-depth ratio (3 levels); C) “warping” of the building shape (3 levels); D) translation along the East-Wast axis (3 levels); E) translation along the North-South axis (3 levels); F) rotation of 180° in steps of 45° (5 levels); G) variation of window width (3 levels); H) variation of insulation thickness - from 2 to 22 cm of glasswool (3 levels).

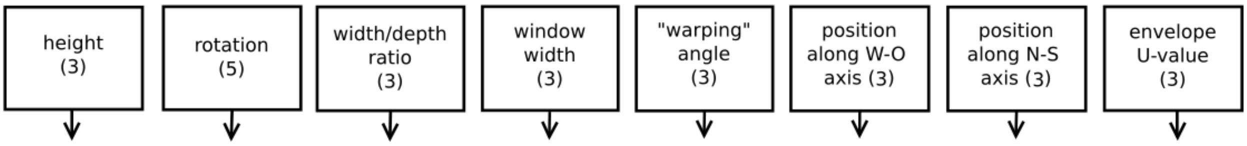

Fig. 5. Parameters and parameter levels in the reference design space.

The total number of iterations of a full-factorial multilevel search were 10965 for the two full-scope models (involving 8 parameters) and 3655 for the two reduced-scope ones (involving 7 parameters). Invariant construction features were: (a) walls: two layers of brick 12cm thick enclosing the insulation; (b) roof: gypsum 1.2cm, honeycomb brick 12cm, reinforced concrete 5cm, glasswool 12cm, air cavity 5cm, aluminium sheets 3mm; (c) ground floors: 6 layers of earth 25cm, gravel 10cm, reinforced concrete 10cm, glasswool 10cm, light concrete 7cm; (d) partitions: gypsum plaster 1.2cm, honeycomb brick 9cm, gypsum plaster 1.2cm.

The air-change rate was set to 1 ach, the casual thermal gains were set to 0, and the climate data of Milan (45 °N, Italy) were utilized.

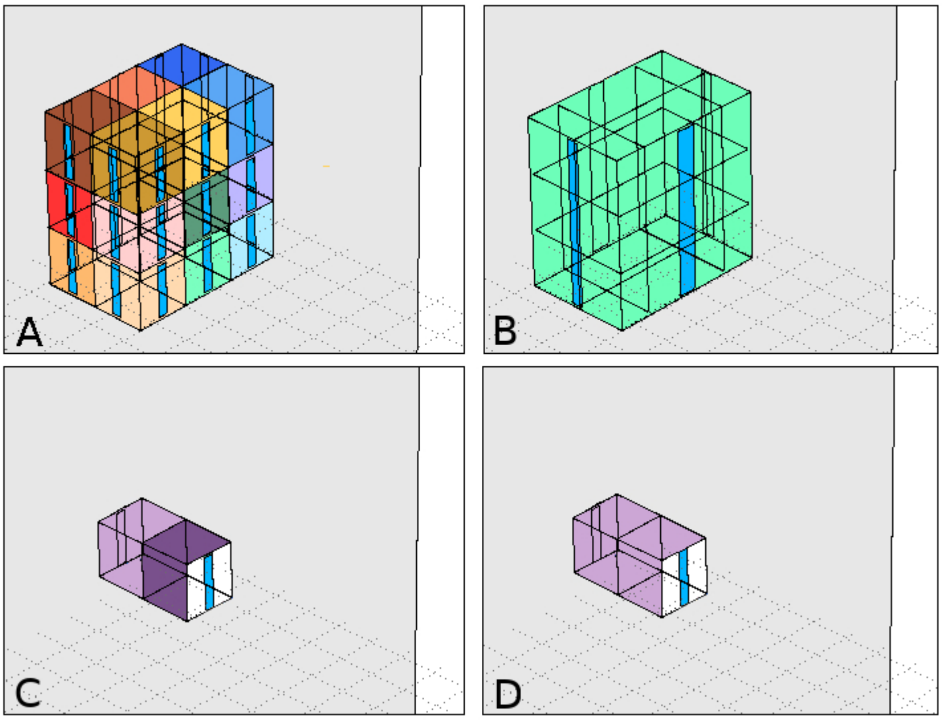

Fig. 6. View of the four building models involved in the explorations. A) Full-scope detailed; B) full-scope simplified; C) reduced-scope detailed; D) reduced-scope simplified. The boundary conditions coloured in violet in models C and D (which regard the surfaces shared among zones) are set to adiabatic.

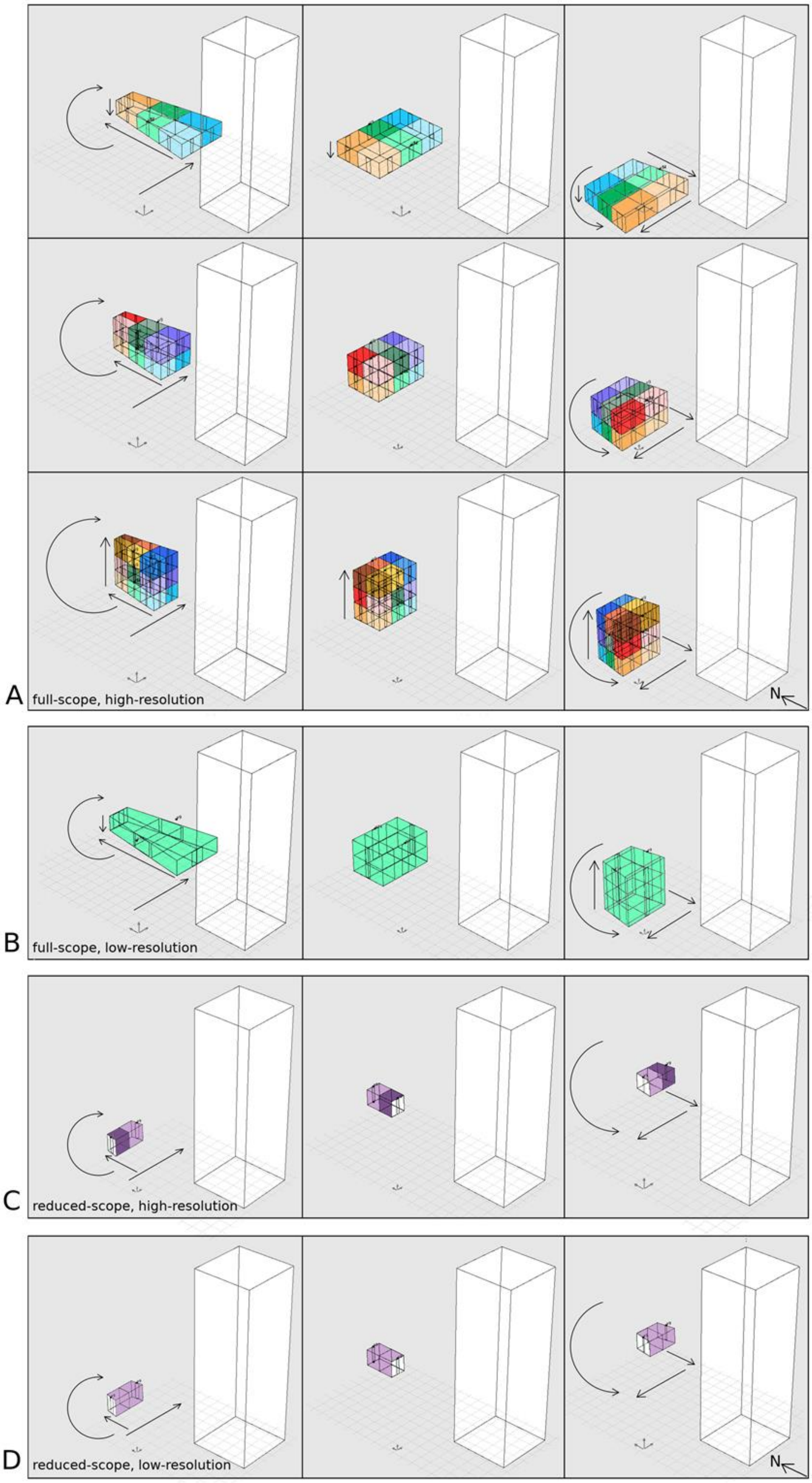

Fig. 7. Some of the transformations involved in the explorations performed in the trials. A) full-scope detailed model; B. full-scope simplified model; C) reduced-scope detailed model; D) reduced-scope simplified model. Each

thermal zone has been given a colour of its own. The boundary conditions coloured in violet in the reduced-scope models C and D (which regard the surfaces shared among zones) are set to adiabatic.

2.8. Trial criteria

The performances of the scene-models have been simulated by the means of a state-of-the-art energy simulation tool, ESP-r (Clarke, 2001; Hand, 2018), managing the optimization and metamodelling operations with the application Sim::OPT (Brunetti, 2008-2019).

The performances obtained from a full-factorial search based on the full-scope detailed scene-model were assumed as a reference, and the predictive reliability of each considered instance was calculated in terms of the deviations of objective performance from them. Predictive reliability was measured as the normalized average of the predictive performance rankings of the 12 most performant instances (NPPR) (12 being the size of a 2-parameters subspace).

Calculating the NPPRs entailed the following steps:

1) ordering the performances of the surrogate model instances from the highest to the lowest by assigning to each a decreasing ranking value, $\mathrm{rank}_{\mathrm{surr}_i}$ (where *i* is the iteration number);

2) forming a set of the *i*-indices of the *m* top-ranked surrogate instances:

$\mathrm{SurrRanks}=\{i_m | m \in \mathrm{N}, 1<m<12\}$, with m =12;

3) ordering the performances from the highest to the lowest and assigning to each a decreasing ranking value, $\mathrm{rank}_{\mathrm{mod}_i}$;

4) finding the average of the $\mathrm{rank}_{\mathrm{mod}_i}$ rankings corresponding to the *i*-indices contained in SurrRanks:

$\mathrm{avgrank}_{\mathrm{surr}} = \frac{\sum_{i \in \mathrm{SurrRanks}} \mathrm{rank}_{\mathrm{mod}_i}}{m}$;

5) normalizing the average ranking, $\mathrm{avgrank}_{\mathrm{surr}}$, with respect to the top ranking:

$\mathrm{NPPR}= \frac{\mathrm{avgrank}_{\mathrm{surr}}}{n}$, where *n is* the total number of instances (10965 in the full-scope model and 3655 in the reduced-scope one).

The procedural trails could vary as regards scene-model type (detailed or simplified, full-scope or reduced-scope), metamodelling strategy (absent or present, and aimed at the whole design-space or at the subspaces) and the search strategy (which could utilize some alternative block-coordinate descent schemes). The amount of descriptive information in each procedural trail was measured as that contained in the description of a scene-model times the number of samples (simulations):

$$I=\sum Im_i * ns \ , \quad (1)$$

where:

Im_i: amount of descriptive information embodied in a scene-model at iteration i.

ns = number of sampled instances.

The criteria for measuring the descriptive information were kept extremely cautious, hypothesizing that an addition of one vertex, one surface, one connection, or one zone produced the same information increase.

The criterion adopted to calculate the amount of information embodied in a scene-model was the following:

$$Im_i = \sum v_i + \sum z_i + \sum s_i \ , \quad (2)$$

where:

Im_i: amount of information in the scene-model at i;

number of vertices;

number of zones;

number of surfaces.

In the cases in which the scene-model transformations did not take place in conditions of constant configuration, the average amount of information embodied in the model along the transitional steps was taken into account (Table 1, Fig. 11).

Table 1. Size of the descriptive information calculated for the scene-models

	1A. full-scope detailed, 1-story	**1B. full-scope detailed, 2-stories**	**1 C. full-scope detailed, 3-stories**	**2. full-scope simplified**	**3. reduced-scope detailed**	**4. reduced-scope simplified**
vertices	94	188	282	46	26	22
surfaces	46	92	138	20	14	10
connections	46	92	138	20	14	10
zones	6	12	18	1	2	1
Total	204	408	612	87	56	43

The comparisons between the outcomes of the procedural trails were based on (a) the NPPRs and (b) an indicator of exploration efficiency constituted by the normalized return on investment in descriptive information in terms of predictive reliability (ROIIPR), calculated on the basis of the NPPRs, then normalized against the optimal results of the full-scope simplified model:

$\mathrm{ROIIPR}_i = \frac{\mathrm{roiipr}_i}{\mathrm{roiipr}_{\mathrm{maxFSS}}}$,

where:

$\mathrm{roiipr}_i = \frac{\mathrm{NPPR}_i}{I}$: non-normalized return on investment in information at *i*;

I: amount of descriptive information in the search-trail;

NPPR_i normalized predictive performance ranking of instance *i*;

$\mathrm{roiipr}_{\mathrm{maxFSS}}$: maximum non-normalized ROIIPR recorded in the design-space of the full-scope simplified model.

Finally, the rates of change of the ROIIPRs from one step of the procedural trail to another were calculated.

The described grafting procedure can be utilized without any addition when the sampling of the design spaces is complete. But when it is incomplete, it must be preceded by a metamodelling phase, to determine the performances of the unsampled vectors. And because the present trials were aimed to exploit descriptive information efficiently, the sampling was set to be partial, and a metamodelling phase was scheduled.

Several candidate metamodelling procedures were considered for performing the metamodelling task (Fig.8). The choice fell on the same distance-weighted gradient-based procedure (DWGN) already utilized for the grafting operations, combined with an ad-hoc sampling strategy based on clouds of star samplings distributed semi-stochastically (Brunetti, 2019; Brunetti, 2018-2019). The predictive reliabilities of the considered metamodelling procedures showed a range of variation much smaller than that deriving from the procedures utilizing grafting and procedures not utilizing it. In any case, the chosen metamodelling procedure produced the highest predictive rankings and could be integrated with block-coordinate descent optimization.

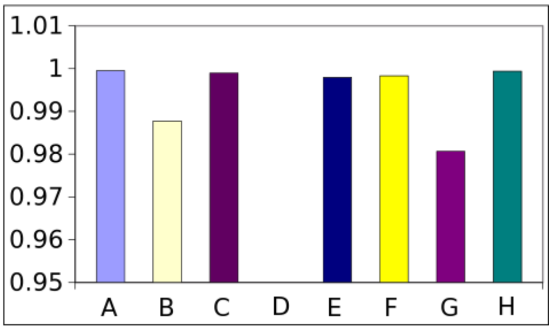

Fig. 8. Normalized predictive performance rankings (NPPR) of the candidate metamodelling procedures. Legend. A) reference (full-factorial); B) polynomial, 1st order; C) polynomial, 2nd order; D) polynomial, 3rd order (failed); E) kriging; F) MARS; G) ANN; H) DWGN.

The grafting technique was tested by grafting some subspaces of the full-scope simplified metamodel into the subspaces of a reduced-scope one. The operation was performed conformingly to the procedure presented in section 2.1, and in constant design-space-model configuration. This was obtained by assigning to the reduced-scope metamodel the dummy parameter “height” (set to 3 stories), and, optionally, by substituting the vectors deriving from “warping” and/or “rotation” with dummy ones; which in turn was obtained by stripping away from them the performances not pertaining their central levels (chosen, respectively, as 0° and “South”) (Fig. 9B).

The settings entailed that one of the two reduced-scope design-space models (detailed or simplified) was assumed as the “backbone” to which the simplified full-scope model contributed the gradients for deriving the new points. The reason why the full-scope model was here chosen as a donor and the reduced-scope one was chosen as a receiver is that the vectors contained in the reduced-scope space were a subset of those contained in the full-scope one. But in situations in which the overlap between the two design-spaces is partial, and no design-space is completely contained in another, the donor/receiver choice depends on the aims of the analyses and the features of the design spaces. A typical situation is that a reduced-scope donor space contributes information derived from specialized analyses to the receiver. In this case, if both the receiving and the donor space have been populated from the start with all the vectors, importing the information from the donor space into the receiving one would require progressively applying the donor-space gradients to the known vectors in the receiving space. But when, like in the case in question, the vectors in the two spaces have been only partially sampled, the missing information has to be filled in by metamodelling, before the grafting operations. Here, this has been done utilizing DWGN metamodelling procedure, which is based on the same gradient-based technique of the grafting procedure, and additionally entails that each unknown vector is derived by distance-weighting all the available concurrent candidate coordinates (Brunetti, 2019).

The choice of “height”, “warping angle” and “rotation” as parameters to be grafted was made because the reduced-scope models (Fig.7C and 7D) could not take into account variations in height and were at risk of producing inadequate responses when modelling warping and rotation, due to the proportions of their shape and to the adiabatic conditions of many of their boundaries.

Fig. 9. Some of the grafting tactics utilized in the case study. A) Grafting by substitution of the design subspaces regarding the “height” and “rotation” of a full-scope design space model onto a reduced-scope one; B) the same as A, but as regards the parameters “height”, “warping angle” and “rotation”.

The outcomes of the information reduction made possible by grafting have then been compared with the outcomes of combining scene-model reduction and metamodelling with overlapping block-coordinate descent (BCD), considering the suitability of BCD to model cascaded searches. The following search strategies have been tried:

a) a strategy not entailing metamodelling, but performing the descents directly on the design-space models (Fig. 10A1-A3);

b) a strategy sampling the whole extension of the design-space, creating a whole-space metamodel upfront from that sample, then dividing it into subspaces, and finally performing the descents on those subspaces of metamodel (Fig. 10B2);

c) the strategy of subspace metamodelling: subdividing the design-space into subspaces, then sampling, metamodelling and searching each subspace sequentially on the basis of the results of the previous search (Fig. 10C1-C2). This strategy limits the size of metamodels and reduces both the computational load of the metamodelling operations and the error they produce. Other advantages of this strategy are that, everything else being equal, it requires fewer samples than the one entailing the creation of a whole-space metamodel followed by the subdivision into subspaces (Fig.10B2), and is computationally lighter, due to the smaller size of the metamodels.

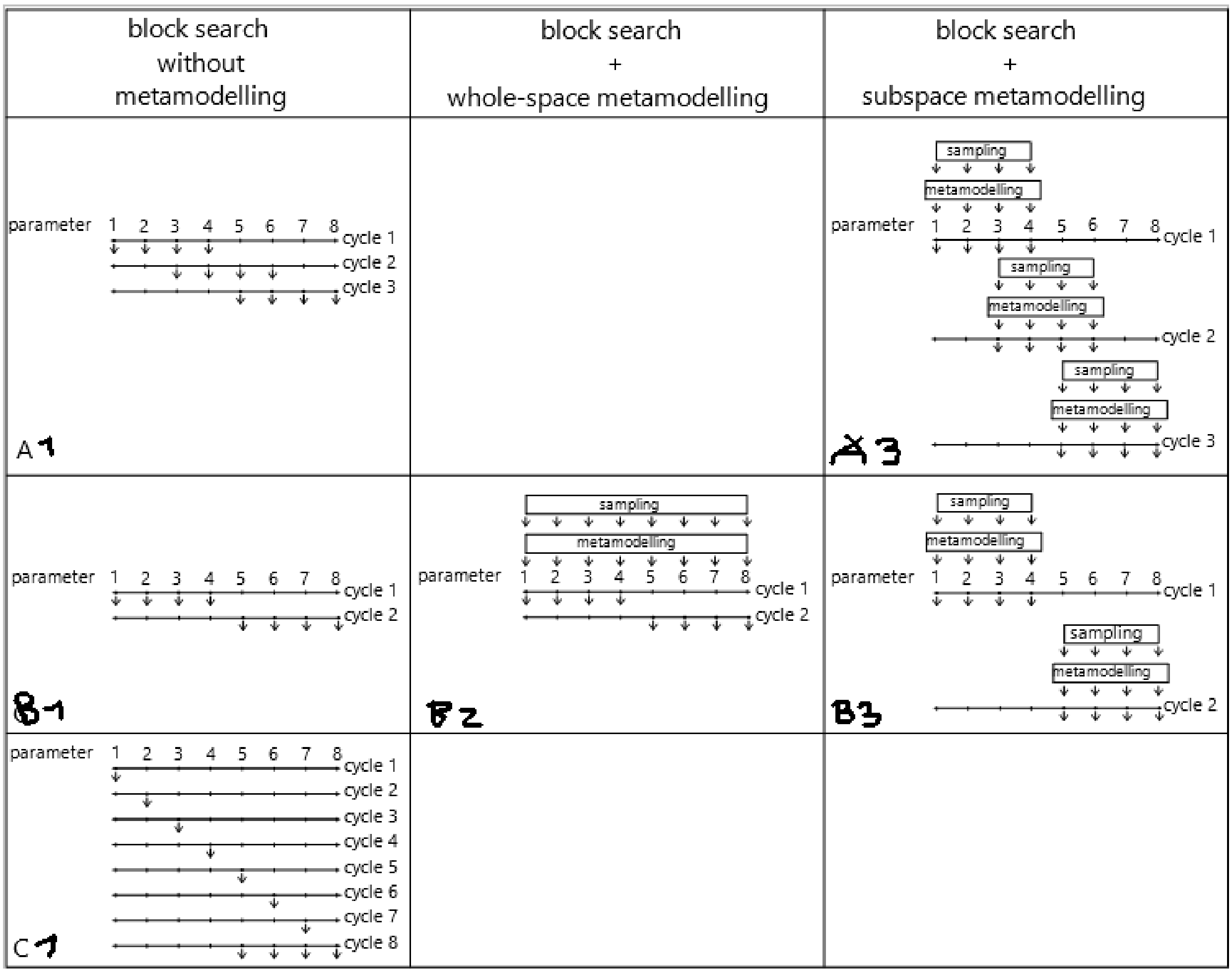

Fig. 10. Schemes of the block-coordinate searches taken into account. A1) descent on overlapping subspaces of model; B1) descent on subspaces of model; C1) descent on tiny subspaces of model; B2) descent on subspaces of metamodel; A3) descent on overlapping metamodels of subspaces; B3) descent on metamodels of subspaces.

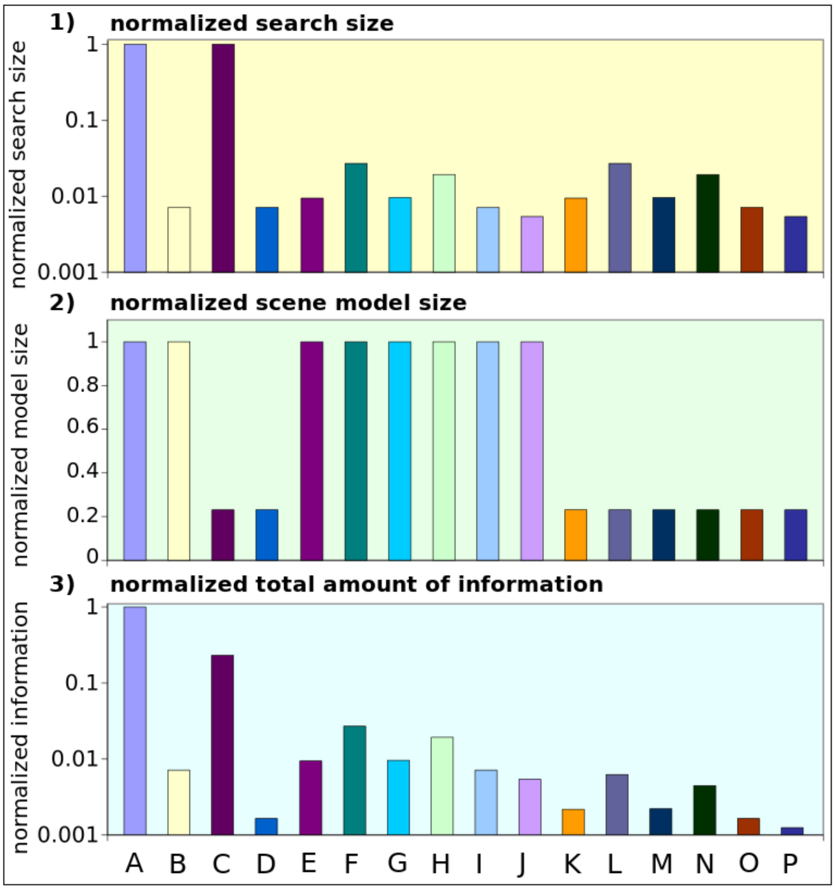

Fig. 11. 1) Amount of information relative to the search sizes; 2) amount of information in the scene models; 3) amount of information relative to the procedural trails. The letters and numbers assigned to each case are the same as Fig. 9. Legend: DM; detailed model; SM: simplified model. Cases: A) DM; B) DMm; C) SM; D) SMm; E) C1, from DM; F) A1, from DM; G) A3, from DM; H) B1, from DM; I B2, from DM; J) B3, from DM; K) C1, from SM; L) A1, from SM; M) A3, from SM; N) B1, from SM; O) B2, from SM; P) B3, from SM.

To reduce the role of chance in the choice of the parameter sequences (Fig.10), the exploration strategies in question were tested by averaging the results derived from utilizing 5 different sequences of parameter numbers cast randomly - the same for each case. That this was due, can be seen in Fig.15, which shows the diversity of outcomes deriving from 4 different stochastic samples.

3. Results

The main information that emerged from the trials is that grafting a part of a full-scope simplified design-space metamodel onto a reduced-scope metamodel produced in all cases impressive returns on investment of information (ROIIPRs) (Fig.12-2), substantially higher than the highest ones obtained without grafting (Fig.13-2) and greater the greater was the reduction level of the receiving design-space. But it also emerged that when both the donor space and the receiving one were low-resolution, grafting could produce low predictive reliability (NPPR). Indeed, when the full-scope detailed model was the donor, the NPPRs fell from about 90% to about 80% after exchanging the reduced-scope detailed metamodel for the reduced-scope simplified one (Fig.12E-H versus Fig.12M-P) as a receiving space. However, when the full-scope simplified model was the donor, the difference between receivers did not emerge (Fig.12I-L versus Fig.12O-T): the donor did not strongly influence predictive reliability if the receiver was not high-quality.

As regards the relation between the quantity of grafted subspaces and predictive performances, the more was not always the better. The improvements in the NPPRs and ROIIPRs did not indeed occur monotonically. The NPPR of both possible receivers were substantially higher when the donor was the detailed full-scope metamodel rather than the simplified one; and their returns peaked with the graft of “height” plus “warping angle” (Fig. 12J, 12L), but decreased when “rotation” was donated. Enlarging the number of donated parameters beyond 2 produced no benefit (Fig.12K-L versus 12J, 12S-T versus 12R).

At a general level, the trials showed that the amount of information utilized to describe an exploration can be reduced efficiently by distributing it among procedural levels: scene-model, design-space and search.

Scene-model reduction was a major component of the grafting technique; but by itself, it produced non-impressive returns (ROIIPRs) (Fig.13-2), due to low predictive reliability (NPPRs) (Fig.13-1). On the other hand, it turned out to be a robust strategy, combinable with metamodelling and decomposition without altering the rates of change of the ROIIPRs: a clue of its suitability to support design decisions based on relative rather than absolute considerations (Fig. 14-2).

Metamodelling produced a significant increase in the returns (Fig.13-2) and showed to be useful both in combination with the detailed scene-models and with the simplified ones, and both in subspace searches performed on full-scope metamodels and on reduced-scope ones: the information reductions obtained were huge, more than one hundredfold. And the block-searches showed that high returns could also be obtained from search structures characterized by small subspaces sharing small or no overlaps (Fig.10A2, Fig.13-2).

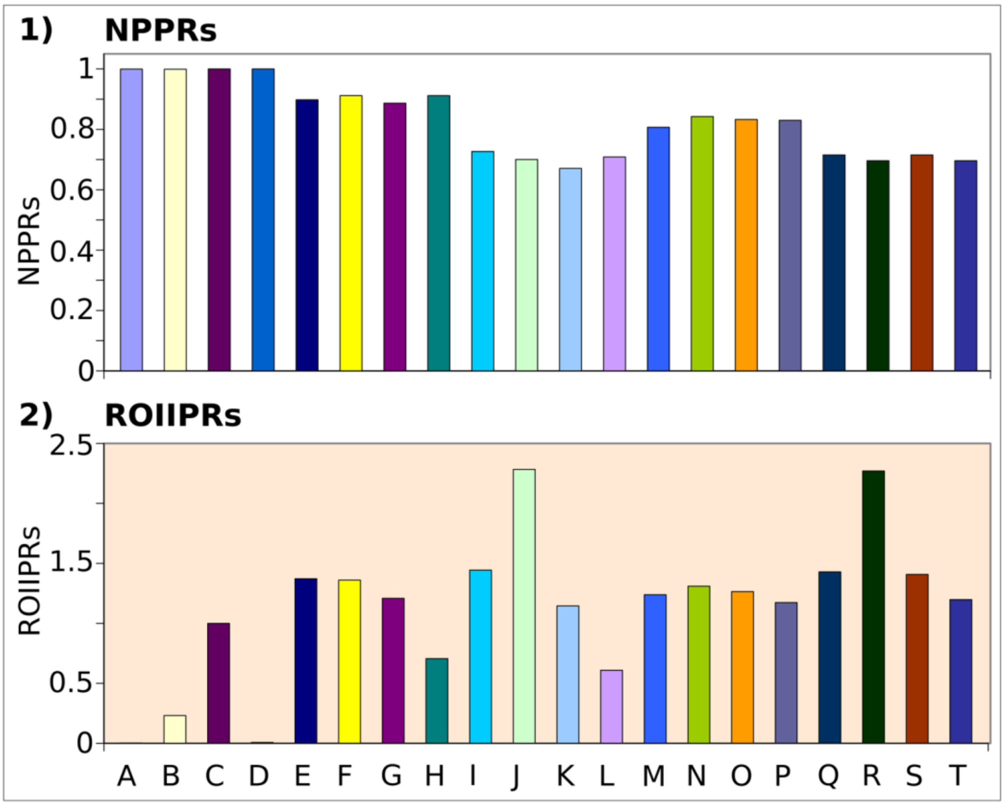

Fig. 12. 1) NPPRs of the top performing instances deriving from the full-factorial search “trails” (A-D) and from grafting the parameters “height” (“H”), “warping angle” (“W”) and “rotation” (“R”) of the full-scope detailed metamodel (FDMm: B) or of the simplified metamodel (FSMm: D) into the reduced-scope detailed metamodel (RDMm) or into the simplified metamodel (RSMm). 2) ROIIPRs. Cases: A) FDM; B) FDMm; C) FSM; D) FSMm; E) graft of “H” of FDMm in RDMm; F) “H” and “W” of FDMm in RDMm; G) “H” and “R” of FDMm in RDMm; H) “H”, “W” and “R” of FDMm in RDMm; I) “H” of FDMm in RDMm; J) “H” and “W” of FDMm in RDMm; K) “H” and “R” of FDMm in RDMm; L) “H”, “W” and “R” of of FDMm in RDMm; M) “H” of FSMm in RDMm; N) “H” and “W” of FSMm in RDMm; O) “H” and “R” of FSMm in RDMm; P) “H”, “W” and “R” of FSMm in RDMm; Q) “H” of FSMm in RDMm; R) “H” and W of FSMm in RDMm; S) “H” and “R” of FSMm in RDMm; T) “H”, “W” and “R” of FSMm in RDMm.

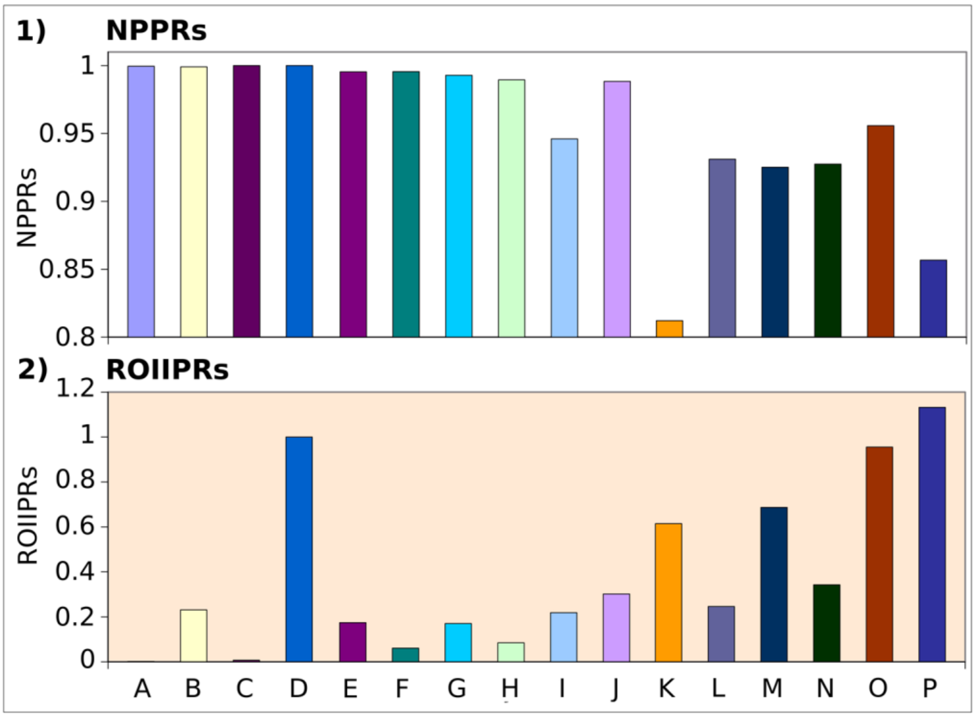

Fig. 13. 1) NPPRs of the 12 top performing instances deriving from the full-factorial search trails (A-D) and from the instances involving block search. 2) ROIIPRs deriving from the same strategies. The letters and numbers assigned to the each case are the same as Fig. 9. Legend: detailed model: DM; simplified model: SM. Cases: A) DM; B) DMm; C) SM; D) SMm; E) C1, from DM; F) A1, from DM; G) A3, from DM; H) B1, from DM; I B2, from DM; J) B3, from DM; K) C1, from SM; L) A1, from SM; M) A3, from SM; N) B1, from SM; O) B2, from SM; P) B3, from SM.

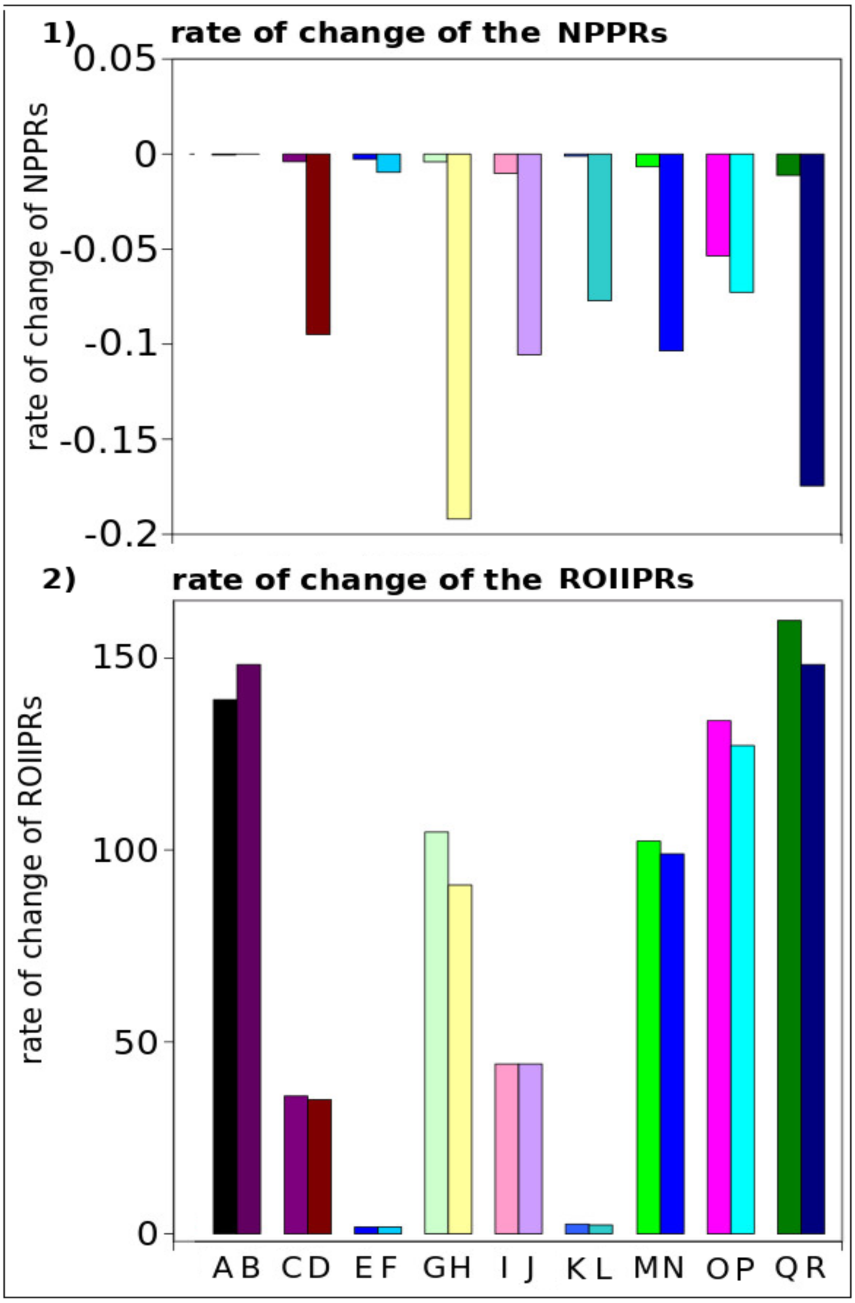

Fig. 14. 1) Paired comparisons of the rates of change of the NPPRs from the full-factorial search “trails” (A-D) to the “trails” involving block search. The left column of each pair derives from the ratio between two full-scope detailed models and the right column of each pair derives from the ratio between two full-scope simplified models. The letters and numbers assigned to the each case are the same as Fig. 9. 2) Analogue pair comparisons of the rates of change of the ROIIPRs. Legend: full-factorial: FF; detailed model: DM; simplified model: SM. Cases: A) FFDM / FFDMm; B) FFSM / FFSMm; C) FFDM / A1 from DM; D) FFSM / A1 from SM; E) A1 from DM / A3 from DM; F) A1 from SM / A3 from SM; G) FFDM / C1 from DM; H) FFSM / C1 from SM, I) FFDM / A1from DM; J) FFSM / A1from SM; K) A1 from DM / A3 from DM; L) A1 from SM / A3 from SM; M) FFDM/ A3 from DM; N) FFDM/ A3 from DM; O) FFDM / B2 from DM; P) FFSM / B2 from SM; Q) FFDM / B3 on DM; R) FFSM / B3 from SM.

4. Discussion

4.1 Scene-model reduction

The fact that scene-model reduction, which is a premise of design-space grafting, is well-suited to be combined with the other reduction strategies without distorting the curvatures of design-spaces can be verified in the rates of change of the returns on investment of information (ROIIPRs) between procedural “nodes” along the search-trails involving scene-model reduction: in Fig.14-2, it can be seen that the rates of change of the ROIIPRs derived from the full-scope detailed models (left columns of each pair) and those derived from the simplified ones (right columns) never diverged substantially, despite strong divergences in predictive reliability (NPPR) between search-trails (14-1). This suggests that scene-model reduction can be confidently utilized for taking design decisions on the basis of relative considerations, comparisons. Similar rates of change of the ROIIPR between different search structures are shared by scene-models of different resolution – like, indeed, the full-scope detailed model in Fig. 7A and the full-scope simplified model in Fig. 7B.

4.2 Grafting

Subspace grafting produced important information reductions, but increasing the quantity of surrogation embodied in it beyond certain levels deteriorated the NPPRs: indeed, while the ROIIPRs derived from performing grafting on the reduced-scope simplified metamodel (Fig. 12-2, M-T) were on average higher than those derived from the detailed model (Fig.12-2, E-L), the NPPRs were substantially lower (see Fig.12-1, M-T versus Fig.12-1, E-L). The decrease in the ROIIPRs obtainable by overlaying surrogation over surrogation emerged also in the lack of substantial differences in NPPRs between the reduced-scope detailed metamodel and the simplified one when the graft donor was the full-scope simplified metamodel: the implication is that the firmer is the ground onto which a graft is implanted, the better the predictions.

The predictive performance reduction deriving from injecting and excessive amount of surrogation into grafting may have been favoured by two circumstances: (a) the NPPRs of the design-space models from which the metamodels of the receiving spaces were modelled were substantially lower than those of the full-scope models; (b) not all the donated parameters had the same level of usefulness performance-wise: “warping” had a higher return on investment than “rotation”, because it was structured in fewer parameter levels, and therefore entailed smaller sampling costs. Moreover, the quality of the predictions produced by the reduced-scope scene-models regarding rotation were already satisfactory in the first place, due to to the adiabatic boundaries; and also, the fact that the average shapes of the donor scene-models were fairly compact did not contribute to differentiating the performances in relation to orientation.

In any case, a substantial part of the grafting experiments attained a high level of predictive reliability, despite the fact that many combinations of solutions had not been tried. This is no proof, but it shows that the grafting technique can be up to the task of making it possible to merge design solutions at the level of design-space models rather than at that of performances, so as to make the mutual alignment of design-space models unnecessary at the root.

As regards the predictive reliability that may be demanded in a design exploration: because predictive reliability is usually a requirement, the NPPR could be set as a threshold. And along the same line, because the returns on investment of information are likely to be an objective, ROIIPRs could be interpreted as a continuum with no threshold, such that the lower, the better. An appropriate procedural strategy could be, therefore, picking the search trail producing the highest ROIIPRs among those having an NPPR above the threshold. In the case in question, if the NPPR threshold had been set to 0.9 (90%), the most advantageous choice would have been that of case F in Fig.12 (entailing grafting “height” and “width” of the full-scope detailed model –Fig.6A- into the reduced-scope detailed model –Fig.7C), which shares the same level of returns on investment as 12N (same donor and donation, and the reduced-scope detailed model as receiver: Fig.7D), but has a substantially lower predictive reliability. In that case, also the highest ROIIPRs coincide with low levels of NPPR (Fig.12J, 12R).

4.3 Combining decomposition and metamodelling

The trials also showed the advantages of combining scene-model reduction, design-space metamodelling and search-path reduction-by-optimization. Most of the search-trails taken into account, with the exception of those entailing decompositions in tiny subspaces (Fig.13D, 13K) or metamodelling reduced-scope simplified scene-models (Fig.13O, 13P) produced high NPPRs, well above 80%. This suggests that optimization (here, decomposition-based optimization) can be used both as an alternative to metamodelling and in combination with it to pursue information reduction. An increase in the ROIIPRS at the cost of a slight decrease of the NPPRs was indeed obtained both when decomposition-based optimization was used by itself (Fig.13E, 13F, 13H), and when it was used to “seed” metamodelling (from 13E to 13P).

Metamodelling the whole design-space upfront, and then searching into its subspaces was shown to be advantageous for producing information both about the optimal solutions and about the design-space shape; while metamodelling the subspaces turned out to be more efficient as regards optimization, but less suited to produce knowledge about the design-space shape. This can be seen in Fig.16: the results of the search-trail in the former case converged towards the reference since the first search cycle, while in the latter, they did only at the second (and last) cycle. The overall predictive reliability derived from a block-search on subspace metamodels can indeed be lower than a block-search on a whole-space metamodel (Fig.13-1O, 13-1P) even when the ROIIPRs are higher (Fig.13-2O, 13-2P): in the former case, the transmission of information between subspaces is the only operation in which some of the curvatures into play between the borders dividing the active and the inactive parts of each subspace can bring their influence onto the search (Fig.17).

Basing a search on subspace metamodels produced the advantage of reducing the relevance of the errors introduced by the metamodelling operations (because it made the metamodels smaller) and lowered the computational investment. But it also left the task of preserving the relations between the different metamodelled design-space zones to the transmission of information taking place within the cascaded search process. By sampling and metamodelling the subspaces one by one, the curvatures existing between the performance of instances located in different subspaces get indeed lost, but they re-emerge as outcomes of the transmission of information taking place in the search at the overlaps (or shared instance) between subspaces.

As always, subdividing a space in block-descent requires balancing the differences between subspaces (assuring search efficiency – like in Fig.10C1-13E) and the commonalities between them (assuring the transmission of information from a subspace search to the next, like in the cases Fig.10A1-13F and Fig.10A3-13G) (Brunetti, 2016). The fact that the predictive reliability deriving from subspace metamodelling was here satisfactory also with no overlaps (like in Fig.10B3-13J) took place in the context of the fact that block-search on subspace metamodels settles optimally only the curvatures of the last-searched subspace, not those of the earlier-searched ones. The strategy of "cascading" a search on the basis of subspace metamodels is indeed only suited to metamodel the space of the optimal and near-optimal instances, and not the whole design-space, because the results of the explorations based on subspace metamodels are quality-skewed towards the optimal solutions. The reason why block search on subspace metamodels works is, therefore, that, even when the curvatures between subspaces are not well detected in the absence of overlaps, the subspace searches are "launched" towards the "right", hopefully-optimal directions because each subspace search takes place on the basis of the optimal solution of the previous one (Fig.16). In other words, the reason is not that the procedure adds the missing curvatures to the design-space model, but that it lets the subspace searches be "cast" in the directions of those curvatures.

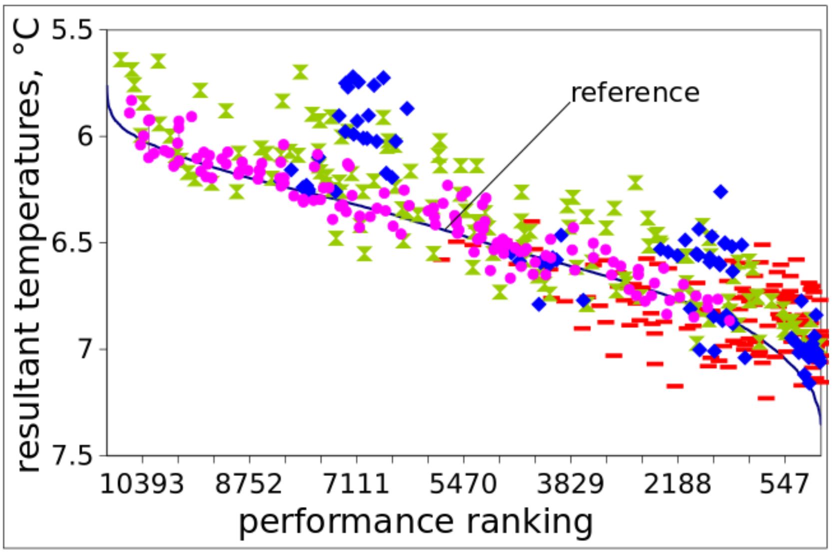

Fig. 15. Example of outcomes of the block-coordinate descent based on partial metamodels, of the type shown in Fig. 13I, focusing on the consequences of stochastic sampling. Continuous line: the reference data series, ordered by performance (resultant temperatures, °C). In 4 colours: the instances of 4 block coordinate descents which have been averaged for returning the value shown in Fig. 11I. The temperature scale has here been inverted to make the maximization problem look like a minimization one, and the best performances have been plotted towards the right and bottom of the graph. The graph must therefore be read from left to right: the rightmost datum is the search outcome.

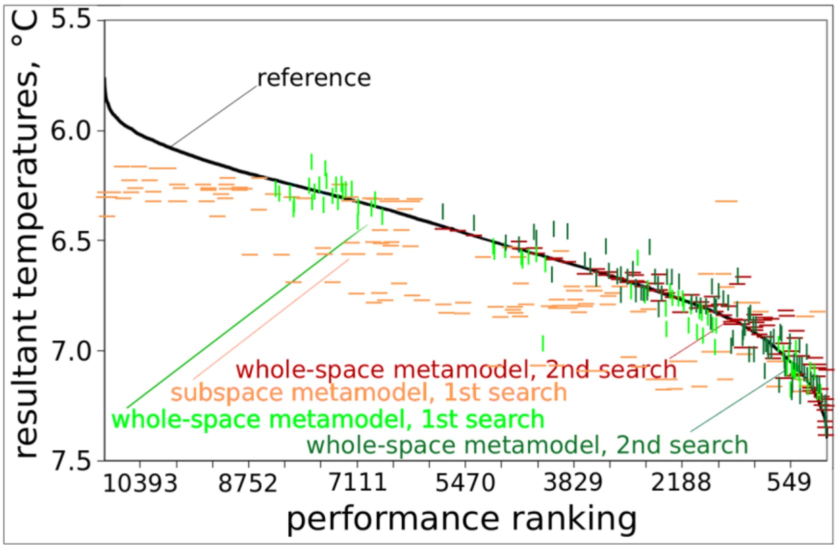

Fig. 16. Example comparing the resultant temperatures collected in a block-coordinate descent based on 2 non-overlapping subspaces of 4 variables when performed on the multi-zone metamodel (case Fig. 10B2) and on subspace metamodels (case Fig. 10B3). The outcomes of the first search cycle are shown in clear colour, and those of the second search cycle are shown in dark colour. The plot follows the same criteria as Fig. 15.

4.4 Cascading the search phases

The trials have also shown that: (a) both the strategies involving operations on scene-models and those involving operations on design-space models can benefit from the fact that the transformations take place in conditions of constant configuration; (b) a combination of constant and variable configuration is the premise for utilizing grafting and cascaded search synergistically. Decomposition-based search benefits indeed from the fact that the topological transformations relative to the scene-model domain are concentrated between constant-configuration search phases; and subspace grafting makes it possible to unify the involved scene-models under a constant configuration obtained at design-space model level. This, in turn, opens up the possibility of combining decomposition-based search and grafting of design-space models of different scope or resolution, so as to make diversity between scene-models at different search states possible even without resorting to scene-model transformations in variable configuration. This means that, while, for example, limiting the reduction strategies to scene-models domain would make it possible to base a cascaded search on a full-scope simplified model (like that in Fig. 6B) and then on a full-scope detailed model (like that in Fig .6A), extending the reduction strategies to the design-space domain through grafting would make possible to chain a search-phase based on a full-scope (detailed or simplified) model (Fig.6B) with one based on a reduced-scope one (like those in Fig.6C and 6D), provided that the models have been represented with the same parameter structure.

By subdividing the search into discrete blocks, sequential decomposition makes it possible that not only transformations regarding the search path can take place between search phases, but also transformations regarding the scene models, involving increases and reductions of scope. This strategy requires performing transformations in constant configuration within the subspaces and frees the search from the necessity of a configurational correspondence between the two "ends" (start and arrival) of a configurational "leap", transformation.

4.5 Multidomain inquiries

All the here presented trials were limited to the thermal domain, but the approach in question could also allow for multidomain analyses. The condition required for that would be the existence of multi-domain performance context shared by all the models. In an operation aimed to grafting a “specialized” design-space model (involving, for example, high-resolution simulations regarding some specific performance domain – solar radiative, lighting, acoustic...) into an all-purpose, generic model, this would also require creating in the generic model some “handles” of performance information relative to the specific domain, at least as regards one parameter combination. That information would be necessary for “anchoring” the donated information into the generic model via the donated gradients. In other words, the exploration would require the availability of a complete range of the performance information for each model: all models should be sampled, at least partially, as regards their multidomain performances, because the grafting operations require the existence of point-to-point correspondences on the side of design-space models.

5. Conclusions

This paper presents a novel approach to graft a design-space model onto another of different scope and/or resolution. At its core, the operation making this possible is a progressive point-to-point adaptation relaxing the mutual calibration requirements concerning different scene-models. The approach can constitute an alternative or a complement (depending on how it is used) to that of undertaking a preliminary analysis on a high-resolution model to select a reduced number of design parameters onto which to perform a full-factorial multilevel analysis. The here presented approach, thanks to its ability to take into account simultaneous variations of non-reduced sets of parameters, makes it possible to produce design landscapes of a completeness that is difficult to obtain otherwise at the same computational expense; and the features of the specific metamodelling method on which it is based (the distance-weighted gradient-network) entail that the procedure does not necessarily need automation beyond that included in its implementation. The main automation task would remain, indeed, in any case, that of managing the detailed scene-model transformations - which the procedure lightens substantially, in number and complexity; to the point of making the strategy of re-using the samples produced in hand-driven explorations or in sensitivity analyses often sufficient for fully populating a design landscape. The metamodelling-and-grafting procedure and variance-based sensitivity analyses are affine to different sampling strategies (the former “prefers” strikes of contiguous vectors, the latter Latin hypercube samplings), but sampling strategies satisfying the requirements of both can be arranged: for example, “clouds” of star samplings, or hypercube samplings based on pairs of adjacent vectors rather than on isolated vectors.

At the most general level, the here presented trials showed that the grafting technique can produce levels of design-space-model reduction of order comparable with that obtainable from subspace metamodelling by sequential decomposition, and have also highlighted the mutual combinability of the alternative forms of design-space-model reduction taken into account (metamodelling and decomposition), as well as their combinability with scene-model reduction.

By simplifying the task of aligning models of different scope and/or resolution, design-space grafting can increase the efficiency of design-space explorations and opens up the possibility of inspecting a design space on the basis of loosely related models in a manner that is leaner – and also, potentially, more flexible and nuanced – than the alternative one, based on the mutual calibration of models. A great deal remains to be assessed as regards the conditions of integration of the grafting technique in the broadest context, its conditions of applicability, and the level of uncertainty related to the grafting operations; but the present results suggest that a savvy combination of the technique with other information reduction strategies could ultimately make possible (computational costs being equal) to explore wider design spaces, or to utilize higher-resolution simulations.

Striking similarities exist between decomposition-based subspace metamodelling and the subspace grafting technique, which indeed do very much the same thing: they manipulate – fill, extend, substitute, merge – design subspaces. Only, in decomposition-based search, the boundaries between subspaces are drawn on the basis of procedural time (iterations), while in subspace grafting they are drawn on the basis of configurational considerations regarding the design-space. But these are only distinctions deriving from how we represent things.

Subspace grafting, metamodelling, scene-model reduction and search decomposition have in common that they all surrogate something: a simplified scene-model surrogates a non-simplified one; a decomposition-based search surrogates a full-factorial multi-level one; a metamodel surrogates the reference design-space, the original, true, “perfect” one; and the graft of a design-space model surrogates a part of another design-space model, blurring even the distinction between scene-model and design-space model. The ultimate consideration that can be extracted from this situation is that there is no dividing line between the treatment of descriptive information taking place within the contexts of scene-models, design-space models, and information flows related to search, and that, therefore, that information could be managed interchangeably for reducing the overall computational loads entailed by simulations. In this perspective, the different possible levels of problem attack could be seen as components of the procedural trail aimed at the search, and could therefore be treated as constituent parts of the search.

6. Acknowledgments

The author would like to thank the anonymous reviewers for their worthy advice and care.

7. References

Abdelalim, A., O'Brien, W., & Shi, Z. (2017). Data visualization and analysis of energy flow on a multi-zone building scale. *Automation in Construction*, 84, 258–273.

Ahn, K. U., Kim, Y. J., Park, C. S., Kim, I., & Lee, K. (2014). BIM interface for full vs. semi-automated building energy simulation. *Energy and Buildings*, 68, 671–678. DOI: 10.1016/j.enbuild.2013.08.063

Al-Bazi, A., & Dawood, N. (2018). Simulation-based optimisation using simulated annealing for crew allocation in the precast industry. *Architectural Engineering and Design Management*, 14:1-2, 109-126. DOI: 10.1080/17452007.2017.1313721

Altman, N. S. (1992). An Introduction to Kernel and Nearest-Neighbor Nonparametric Regression. *The American Statistician*, 46: 3, 175-185. DOI: 10.1080/00031305.1992.10475879

Asl, M. R., Zarrinmehr, S., Bergin, M., & Yan, W. (2015). BPOpt: A framework for BIM-based performance optimization. *Energy and Buildings*, 108, 401–412. DOI: 10.1016/j.enbuild.2015.09.011

Augenbroe, G. (2019). The role of simulation in performance based building. In: Hensen, J.L.M., Lamberts. R., Eds., *Building Performance Simulation for Design and Operation*, 2nd ed. New York, Spoon Press.

Bellman, R. (1957). *Dynamic Programming*. Princeton: Princeton University Press.

Bertsekas, D. P. (1999). *Nonlinear Programming*, 2nd ed. Belmont, Massachusetts: Athena Scientific.

Bertsekas, D.P. (2017). *Dynamic Programming and Optimal Control*, vol. 1, 4th ed. Belmont, Massachusetts: Athena Scientific. (a)

Bertsekas, D.P. (2017). *Dynamic Programming and Optimal Control*, vol. 2, 4th ed. Belmont, Massachusetts: Athena Scientific. (b)

Björklund, T. A. (2013). Initial mental representations of design problems. Differences between experts and novices. *Design Studies,* 34: 2, 135–160. DOI: 10.1016/j.destud.2012.08.005

Blanchard, B.S., W.J. Fabrycky (2010). *Systems Engineering and Analysis*, 5th ed. New York: Prentice Hall.

Boudjehem, D., & Boudjehem, B. (2017). Improved heterogeneous particle swarm optimization. *Journal of Information and Optimization Sciences*, 38:3-4, 481-499. DOI: 10.1080/02522667.2016.1224467

Breiman, L. (2001). Random forests. *Machine Learning*, 45, 5–32.

Brown, N. C., & Mueller, C. T. (2019). Design variable analysis and generation for performance-based parametric modeling in architecture. *International Journal of Architectural Computing,* 17:1, 36-52. DOI: 10.1177/1478077118799491

Brunetti, G.L. (2019). Increasing the efficiency of simulation-based design explorations via metamodelling. *Journal of Building Performance Simulation*. DOI: 10.1080/19401493.2019.1707875

Brunetti, G. L. (2008-2019). Sim::OPT. Software. http://metacpan.org/pod/Sim::OPT

Brunetti, G. L. (2018-2019). Sim::OPT::Interlinear. Software. http://metacpan.org/pod/Sim::OPT::Interlinear

Brunetti, G.L. (2016). Cyclic overlapping block coordinate search for optimizing building design. *Automation in Construction,* 71, 242–261. DOI: 10.1016/j.autcon.2016.08.014

Cao, H., Qian, X., Chen, Z., & Zhu, H. (2017). Enhanced particle swarm optimization for size and shape optimization of truss structures. *Engineering Optimization*, 49:11, 1939-1956. DOI: 10.1080/0305215X.2016.1273912

Cheng, B., & Titterington, D. M. (1994). Neural Networks: A Review from a Statistical Perspective. *Statistical Science,* 9:1, 2-30.

Choudhary, R., Papalambros, P. Y. & Malkawi, A. (2005). A Hierarchical Design Optimization Approach for Meeting Building Performance Targets. *Architectural Engineering and Design Management*, 1:1, 57-76, DOI: 10.1080/17452007.2005.9684584

Clarke, J. A. (2001). *Energy Simulation in Building Design*, 2nd ed. London: Routledge.

Coakley, D., Raftery, P., Keane, M. (2014). A review of methods to match building energy simulation models to measured data. *Renewable and Sustainable Energy Reviews,* 37, 123–141. DOI: 10.1016/j.rser.2014.05.007

Coakley, D., Raftery, P., Molloy, P., & White, G. (2011). Calibration of a detailed BES model to measured data using an evidence-based analytical optimization approach. *Proceedings of Building Simulation 2011*, 374-381.

Cole, W. J., Hale, E. T., & Edgar, T. F. (2013). Building energy model reduction for model predictive control using OpenStudio. *American Control Conference (ACC)*, 17-19. DOI: 10.1109/ACC.2013.6579878.

Cortes, C., & Vapnik, V. (1995). Support-vector networks. *Machine Learning*, 20:3, 273–297.

Cowan, H. J. Gero, J. S., Ding, G. D., & Muncey, R. W. (1968). *Models in Architecture*. Amsterdam: Elsevier.

Cramer, E.J., J.E. Dennis, Jr., P.D. Frank, R.M. Lewis, and G.R. Shubin (1994). Problem formulation for multidisciplinary optimization. *Siam Journal of Optimization*. 4:4, 754-776.

Crawley, D. B., Hand, J. W., Kummert, M., & Griffith, B.T. (2008). Contrasting the capabilities of building energy performance simulation programs. *Building and Environment*, 43:4, 661-673. DOI: 10.1016/j.buildenv.2006.10.027

Davenport, A. G. (1960). Wind loads on structures. Technical Report, Division of Building Research, National Research Council Canada, Issue 88.

Daverman, R. J., & Sher R. B. (Eds.) (2001). *Handbook of Geometric Topology*. Amsterdam: Elsevier.

Deb, K., Pratap, A., Agarwal, S., & Meyarivan, T. (2002). A Fast and Elitist Multiobjective Genetic Algorithm: NSGA-II. *IEEE Transactions on Evolutionary Computation*, 6:2, 182-197.

De Rosa, M., Brennenstuhl, M., Andrade Cabrera, C., Eicker, E., Finn, D. P. (2019). An Iterative Methodology for Model Complexity Reduction in Residential Building Simulation. *Energies*, 12, 2448. DOI: 10.3390/en12122448

Deng, K., Goyal, S., Barooah, P., & Mehta, P.G. (2014). Structure-preserving model reduction of nonlinear building thermal models. *Automatica*, 50, 1188-1195. DOI: 10.1016/j.automatica.2014.02.009

Dino, I. G. (2016). An evolutionary approach for 3D architectural space layout design exploration. *Automation in Construction,* 69, 131–150. DOI: 10.1016/j.autcon.2016.05.020

Dong, A. (2017). Functional lock-in and the problem of design transformation. *Research in Engineering Design*, 28, 203–221. DOI: 10.1007/s00163-016-0234-3.

Ercan, B., & Elias-Ozkan, S. T. (2015). Performance-based parametric design explorations: A method for generating appropriate building components. *Design Studies*, 38, 33-53. DOI: dx.doi.org/10.1016/j.destud.2015.01.001

Evins, R. (2013). A review of computational optimization methods applied to sustainable building design. *Renewable and Sustainable Energy Reviews,* 22, 230–245. DOI: 10.1016/j.rser.2013.02.004

Faloutsos, P. (2001). Composable controllers for physics-based character animation, *SIGGRAPH '01 Proceedings of the 28th annual conference on Computer graphics and interactive techniques,* 251-260. DOI: 10.1145/383259.383287.

Fishwick, P.A., B.P. Zeigler (1992). A Multimodel Methodology for Qualitative Model Engineering. *Transactions on Modelling and Computer Simulation* 2: 1, 52-81.

Frey, D. D., F. Engelhardt, and E. M. Greitzer. (2003). A role for "one-factor-at-a-time" experimentation in parameter design". *Research in Engineering Design,* 14: 2, 65-74.

Friedman, J. H. (1991). Multivariate Adaptive Regression Splines. *The Annals of Statistics,* 1:1, 1-141.

Gerrish, T., Ruikar, K., Cook, M., Johnson, M., Phillip, M., & Lowry C. (2017). BIM application to building energy performance visualisation and management: Challenges and potential. *Energy and Buildings*, 144, 218-228. DOI: 10.1016/j.enbuild.2017.03.032

Geyer, P. (2009). Component-oriented decomposition for multidisciplinary design optimization in building design. *Advanced Engineering Informatics* 23, 12–31. DOI: 10.1016/j.aei.2008.06.008

Geyer, P., J. Stopper, W. Lang, and M. Thumfart (2014). A Systems Engineering Methodology for Designing and Planning the Built Environment. Results from the Urban Research Laboratory Nuremberg and Their Integration in Education. *Systems* 2, 137-158. DOI: 10.3390/systems2020137

Giunta, A., & Watson, L. (1998). A comparison of approximation modeling techniques - Polynomial versus interpolating models, *7th AIAA/USAF/NASA/ISSMO Symposium on Multidisciplinary Analysis and Optimization*, 392-404.

Goldberg, D. E. (1989). *Genetic Algorithms in Search, Optimization, and Machine Learning*. Boston, Massachusetts: Addison-Wesley.

Gosling, W. (1962). The Design of Engineering Systems. New York: Wiley.

Gouda, M.M., Danaher, S., & Underwood, C. P. (2002). Building thermal model reduction using nonlinear constrained optimization. *Building and Environment*, 37, 1255-1265.

Gralla, E. L., Herrmann, J. W., & Morency, M. (2019). Design problem decomposition: an empirical study of small teams of facility designers. *Research in Engineering Design*, 30, 161-185. DOI: 10.1007/s00163-018-0300-0.

Gu, L. Henderson, H. Feng, W., & Ling, F. (2013). “Virtual Design Studio”—Part 1: Interdisciplinary design processes. *Building Simulation*, 6, 235–251. DOI: 10.1007/s12273-013-0110-2

Gu, L., Henderson, H. Feng, W., & Ling, F. (2013). “Virtual Design Studio”—Part 2: Introduction to overall and software framework, 6, 253–268. DOI: 10.1007/s12273-013-0111-1

Habibi, S. (2017). The promise of BIM for improving building performance. *Energy and Buildings*, 153, 525–548. DOI: 10.1016/j.enbuild.2017.08.009

Hand, J. W. (2015). Strategies for Deploying Virtual Representations of the Built Environment, Energy Systems Research Unit, Department of Mechanical and Aerospace Engineering, University of Strathclyde, Glasgow, UK. http://www.esru.strath.ac.uk/Documents/ESP-r_cookbook_june_2015.pdf

Harding, J. E. (2017). Meta-Parametric Design. *Design Studies*, 52, 73-95. DOI: 10.1016/j.destud.2016.09.005

Hardy, R. L. (1971). Multiquadric equations of topography and other irregular surfaces. *Journal of Geophysical Research*, 76: 8, 1905-1915.

Heidarinejad, M. Mattise, N. Dahlhausen, M., Sharma, K., Benne, K., Macumber, D., Brackney, L., Srebric, J. (2017). Demonstration of reduced-order urban scale building energy models. *Energy and Buildings*, 156, 17–28. DOI: 10.1016/j.enbuild.2017.08.086

INCOSE (2019). Guide to the Systems Engineering Body of Knowledge, version 2.2.

Jabi, W. (2013). *Parametric Design for Architecture*. Laurence King Publishing, London,.

Jin, R., Chen, W., & Simpson, T. W. (2001). Comparative studies of metamodelling techniques under multiple modelling criteria. *Structural and Multidisciplinary Optimization*, 23:1, 1–13.

Jin, R., Zhong, B., Ma, L., Hashemi, A., & Ding, L. (2019). Integrating BIM with building performance analysis in project life-cycle. *Automation in Construction*, 106

Kheiri, F. (2018). A review on optimization methods applied in energy-efficient building geometry and envelope design. *Renewable and Sustainable Energy Reviews*, 92, 897-920. DOI: 10.1016/j.rser.2018.04.080

Kim, D., & Braun, J. E. (2015). A general approach for generating reduced-order models for large multi-zone buildings. *Journal of Building Performance Simulation*, 8:6, 435-448. DOI: 10.1080/19401493.2014.977952

Kim, E. J., Plessis, G., Hubert, J. L., & Roux, J. J. (2014). Urban energy simulation: Simplification and reduction of building envelope models. *Energy and Buildings*, 84, 193-202. DOI: 10.1016/j.enbuild.2014.07.066

Kim, J. B., Jeong, W. S., Clayton, M. J., Haberl, J. S., & Yan, W. (2015). Developing a physical BIM library for building thermal energy simulation. *Automation in Constructio*n, 50, 16–28. DOI: 10.1016/j.autcon.2014.10.011

Kim, J.B., Clayton, M.J., Haberl, J.S. & Yan W. (2016). A framework to integrate object-oriented physical modelling with building information modelling for building thermal simulation. *Journal of Building Performance Simulation*, 9:1, 50–69. DOI: 10.1080/19401493.2014.993709

Koenig, R., &Varoudis, T. (2016). Spatial Optimisations - Merging depthmapX, spatial graph networks and evolutionary design in Grasshopper", *ECAADe*.

Lam, W. M. C. (1986). *Sunlighting as Formgiver for Architecture*. New York: Van Nostrand Reinhold.

Laurent, L., Le Riche, R., Soulier, B. Boucar, P.A. (2019). An overview of gradient enhanced metamodels with applications. *Archives of Computational Methods in Engineering*, 26:1, 61-106

Lewis, R.M., Torczon, V. Trosset, M.W. (2000). Direct search methods: then and now. *Journal of Computational and Applied Mathematics*, 124: 1–2, 191–207.

Machairas, V., Tsangrassoulis, A., & Axarli, K. (2014). Algorithms for optimization of building design: a review. *Renewable and Sustainable Energy Reviews*, 31, 101–112. DOI: 10.1016/j.rser.2013.11.036

Mahan Singh, M., Sawhneya, A., Borrmann, A. (2015). Modular coordination and BIM: Development of rule based smart building components. *Procedia Engineering*. 123, 877-705. DOI: 10.1016/j.proeng.2015.10.104

Matheron, G. (1973). The Intrinsic Random Functions and Their Applications. *Advances in Applied Probability*, 5: 3, 439-468.

Medjdoub, B., & Benzohra Chenini, M. (2015). A constraint-based parametric model to support building services design exploration. *Architectural Engineering and Design Management*, 11:2, 123-136. DOI: 10.1080/17452007.2013.834812

Mingers, J., J. Brocklesby (1997). *Multimethodology: for Mixing Towards a Framework Methodologies*. Omega 25: 5, 489-509. DOI: 10.1016/S0305-0483(97)00018-2

Monari, F., & Strachan, P. (2017). CALIBRO: an R Package for the Automatic Calibration of Building Energy Simulation Models. *Proceedings of the 15th IBPSA Conference*, 848-857. DOI: 10.26868/25222708.2017.224

Myers, H.M., Montgomery, D.C., & Anderson-Cook, C.M. (2009). *Response Surface Methodology: Process and Product Optimization Using Designed Experiments*, 3rd ed. New York: Wiley and Sons.

Nembrini, J., Samberger, S., & Labelle, G. (2014). Parametric scripting for early design performance simulation. *Energy and Buildings*, 68, Part C, 786–798. DOI: dx.doi.org/10.1016/j.enbuild.2013.09.044

Nervi, P. (1954). *Costruire correttamente*, Milan: Hoepli.

Nguyen, A. Reiter, S., & Rigo, P. (2014). A review on simulation-based optimization methods applied to building performance analysis. *Applied Energy*, 113, 1043–1058. DOI: 10.1016/j.apenergy.2013.08.061

Olgyay, A., & Olgyay, V. (1957). *Solar Control and Shading Devices*. Princeton: Princeton University Press.

Olgyay, V. (1959). *Design With Climate: Bioclimatic Approach to Architectural Regionalism*. Princeton: Princeton University Press.

Pedrini, A., Westphal, F.S., & Lamberts, R. (2002). A methodology for building energy modelling and calibration in warm climates. *Building and Environment*, 37, 903–912. DOI: 10.1016/S0360-1323(02)00051-3

Pimmler, T.U., S.D. Eppinger (1994). Integration analysis of product decompositions. *Working papers*, Massachusetts Institute of Technology (MIT), Sloan School of Management, 3690-3694.

Radford, A.D. & Gero, J.S. (1988). *Design by Optimization in Architecture, Building, and Construction*. New York: Van Nostrand Reinhold.

Raftery, P., Keane, M., & Costa, A. (2011). Calibrating whole building energy models: Detailed case study using hourly measured data. *Energy and Buildings*, 43:12, 3666–3679. (b)

Raftery, P., Keane, M., & O'Donnell, J. (2011). Calibrating whole building energy models: An evidence-based methodology. *Energy and Buildings*, 43:9 2356 – 2364. (a)

Reddy, T. A., Maor, I., & Panjapornpon, C. (2007). Calibrating Detailed Building Energy Simulation Programs with Measured Data—Part I: General Methodology. *HVAC&R Research*, 13:2, 221-241. DOI: 10.1080/10789669.2007.10390952. (a)

Reddy, T.A., Maor, I., & Panjapornpon, C. (2007). Calibrating Detailed Building Energy Simulation Programs with Measured Data— Part II: Application to Three Case Study Office Buildings. *HVAC&R Research*, 13:2, 243-265. DOI: 10.1080/10789669.2007.10390953. (b)

Sacks, R., Eastman, C. M., & Lee. G. (2004). Parametric 3D modeling in building construction with examples from precast concrete. *Automation in Construction*, 13, 291–312. DOI: 10.1016/S0926-5805(03)00043-8

Sage A.P. (1992). *Systems Engineering*. New York: Wiley.

Shadram, F., & Mukkavaara, J. (2018). An integrated BIM-based framework for the optimization of the trade-off between embodied and operational energy. *Energy and Buildings*, 158, 189–1205. DOI: 10.1016/j.enbuild.2017.11.017

Shamsi, M. H., Ali, U., & O'Donnell, J. (2017). A generalization approach for reduced order modelling of commercial buildings, Journal of Building Performance Simulation. *Energy Procedia*, 122, 901-906. DOI: 10.1080/19401493.2019.1641554

Simon, H.A (1973). *The Sciences of the Artificial*. Cambridge, Massacusetts, MIT Press.

Simon, H.A. (1962). The architecture of complexity. *Proceedings of the American Philosophical Society*, 106(6): 467-482.

de Souza, C.B. (2012). Contrasting paradigms of design thinking: The building thermal simulation tool user vs. the building designer. *Automation in Construction* 22, 112-122. DOI: 10.1016/j.autcon.2011.09.008

Stevanović, S. (2013). Optimization of passive solar design strategies: a review. *Renewable and Sustainable Energy Reviews,* 25, 177–196. DOI: 10.1016/j.rser.2013.04.028

Sussman, G. J., & Steele, G. L. (1980). Constraints - a language for expressing almost hierarchical descriptions. *Artificial Intelligence*. 14:1, 1–39. DOI: dx.doi.org/10. 1016/0004-3702(80)90032-6

Sussman, G.J. (2007). *Building Robust Systems*. Web document. http://groups.csail.mit.edu/mac/users/gjs/6.945/readings/robust-systems.pdf

Sutherland, & I. E. (1963). Sketchpad, a man-machine graphical communication system, PhD thesis, Massachusetts Institute of Technology.

Sweller, J. (1988). Cognitive Load During Problem Solving: Effects on Learning. *Cognitive Science,* 12, 257-285.

Tang, B., Han, J., Guo, G.F., Chen Y., & Zhang, S. (2019). Building material prices forecasting based on least square support vector machine and improved particle swarm optimization. *Architectural Engineering and Design Management*, 15:3, 196-212. DOI: 10.1080/17452007.2018.1556577

Thompson, D.W (1917-1942). *On Growth and Form*. Cambridge, UK, Cambridge University Press.

Tseng, P. (2001). Convergence of a block coordinate descent method for nondifferentiable minimization. *Journal of Optimization Theory and Applications,* 109: 3, 475–494.

Turk, Ž. (2016), Ten questions concerning building information modelling. *Building and Environment*, 107, 274-284. DOI: 10.1016/j.buildenv.2016.08.001

Turrin, M., von Buelow, P., Stouffs, R. (2011). Design explorations of performance driven geometry in architectural design using parametric modeling and genetic algorithms. *Advanced Engineering Informatics*, 25, 656–675.

van Keulen, F., & Vervenne, K. (2004). Gradient-enhanced response surface building. *Structural and Multidisciplinary Optimization*, 27, 337–351. DOI: 10.1007/s00158-004-0392-1

Villa-Vialaneix, N., Follador, M., Ratto, M., & Leip, A. (2012). A comparison of eight metamodeling techniques for the simulation of N 2 O fluxes and N leaching from corn crops. *Environmental Modelling & Software*, 34, 51-66. DOI: 10.1016/j.envsoft.2011.05.003

Wang, G. G., & Shan, S. (2006). Review of metamodeling techniques in support of engineering design optimization. *Journal of Mechanical Design*, 129:4, 370-380. DOI: 10.1115/1.2429697

Weinberg, G.M. (1975). *An Introduction to General Systems Thinking*. New York: Dorset House.

Welle, B., Rogers, Z., & Fischer, M. (2012). BIM-Centric Daylight Profiler for Simulation (BDP4SIM): A methodology for automated product model decomposition and recomposition for climate-based daylighting simulation. *Building and Environment*, 58, 114-134. DOI: 10.1016/j.buildenv.2012.06.021

de Wilde, P. (2018). Building Performance Analysis. New York, Wiley.

Winston, P. (1992). *Artificial Intelligence*, 3rd ed. Reading, Massachusetts: Addison-Wesley.

Woodbury, R. (2010). *Elements of Parametric Design*. London: Routledge.

Wortmann, T. Tunçer, B. (2017), Differentiating parametric design: Digital workflows in contemporary architecture and construction. *Design Studies*, 52, 173-197.

Wynn, D. C. & Eckert, C. M. (2017). Perspectives on iteration in design and development. *Research in Engineering Design*, 28, 153–184. DOI: 10.1007/s00163-016-0226-3

Yang, D., Ren, S., Turrin, M., Sariyildiz, S., & Sun, Y. (2018). Multi-disciplinary and multi-objective optimization problem re-formulation in computational design exploration: A case of conceptual sports building design. *Automation in Construction*, 92, 242–269. DOI: 10.1016/j.autcon.2018.03.023

Yang, F., & Bouchlaghem, D. (2010). Genetic Algorithm-Based Multiobjective Optimization for Building Design. *Architectural Engineering and Design Management*, 6:1, 68-82. DOI: 10.3763/aedm.2008.0077

Yoon, J.H., Lee, E.J., & Claridge, D. E. (2003). Calibration Procedure for Energy Performance Simulation of a Commercial Building. *Journal of Solar Energy Engineering*, 125, 251-257. DOI: 10.1115/1.1564076

Yu, B. Y., Honda, T. (2016). Human behavior and domain knowledge in parameter design of complex systems. Design Studies, 45, 242-267. DOI: 10.1016/j.destud.2016.04.005